Controls on Geomorphology and Sedimentology of Shoreface-Beach Ridge-Lagoon Systems on a Low-Energy Carbonate Ramp: Holocene, Northwestern Yucatan Shelf, Mexico

By

Jennifer Giselle Lowery

Submitted to the graduate degree program in Geology and the Graduate Faculty of the University of Kansas in partial fulfillment of the requirements for the degree of Master of Science.

_____

Chair: Dr. Eugene Rankey

_____

Dr. Evan Franseen

_____

Dr. Alison Olcott-Marshall

_____

Dr. Rodrigo Garza-Perez

Date Defended: May 12, 2016

The Thesis Committee for Jennifer Giselle Lowery

certifies that this is the approved version of the following thesis:

Controls on Geomorphology and Sedimentology of Shoreface-Beach Ridge-Lagoon Systems on a Low-Energy Carbonate Ramp: Holocene, Northwestern Yucatan Shelf, Mexico

_____

Chair: Dr. Eugene Rankey

Date approved: June 13, 2016

Abstract

Whereas Holocene carbonate accumulations of isolated platforms and rimmed shelves are well-understood, modern carbonate ramps have not been as extensively studied. Yet, many ancient successions consist of fine-grained sediment deposited on low-energy carbonates ramps. To better understand the sedimentologic variability and accumulations of low-energy ramp systems, this project tests the hypothesis that sediment size, sorting and type, and organic matter abundance varies among geomorphic elements on the Holocene ramp system on the northwestern Yucatan shelf, Mexico. Understanding how sediment and organic matter abundance vary in ramp carbonates is important for constructing actualistic depositional models for depositional heterogeneity within their ancient analogs, some of which include prolific hydrocarbon reservoirs.

These results illustrate trends in geomorphology, sedimentology, and organic matter on shoreface-beach ridge-lagoon systems on a low-energy carbonate ramp. In terms of physical oceanographic processes, regional data suggest that currents generated by the day-to-day easterly trade winds, and larger waves caused by winter cold fronts, have the net effect of transporting sediment and upwelled waters southward along the northwestern Yucatan Peninsula. Offshore regions include shore-parallel belts of *Halimeda*-rich muddy gravel and skeletal (mainly molluscan) muddy sand to gravel. Longshore sediment transport along the coast forms barrier island spits made up of molluscan coquina beach ridges, which have prograded southward and westward in a repeated pattern. The barrier islands at Celestun and Isla Arena in turn act as barriers to the offshore wind and wave energy, creating semi-restricted, low-energy lagoons in their lee. These lagoons contain finer sediment (including abundant mud, >20%) and a higher abundance of organic matter (up to 15%). A landward supratidal marsh (the “Petenes”) includes dominantly fine-grained carbonate sediment.

In addition to physical processes, chemical oceanographic factors likely influence the sediment of the area. The presence of upwelled waters containing elevated nutrient levels (>5 mg/m^3, eutrophic to hypertrophic) and cooler water (~17-18°C) shape the assemblage of sediment producers present in the study area. Molluscs are the main sediment contributors in the region, along with *Halimeda* offshore. Barnacles, foraminifera, sponges, bryozoans, and serpulid worm tubes constitute the remainder of carbonate sediment producers. Corals are markedly absent, as are peloids and ooids. Unexpectedly, as the northwestern Yucatan occurs in a tropical ocean, abundant biosiliceous organisms such as diatoms and sponge spicules, as well as some dinoflagellates and coccolithophores, contribute to sediment throughout the offshore and lagoon. This diverse biosilicious assemblage further implicates the influence of nutrients and cool waters on the sediment producers in the area.

The results of this study illustrate physical (energy level, SST) and chemical (upwelled waters) oceanographic influences on the geomorphology and sedimentology of a Holocene ramp system. The insights motivate a conceptual model for the nature and controls on sedimentologic and geomorphic heterogeneity in ancient nearshore, low-energy ramp systems, including some ancient reservoir analogs.

Acknowledgements

This study was funded through the Kansas Interdisciplinary Carbonate Consortium (KICC), and I would like to thank all of the sponsors and their generous support of KU Geology students and their research. Research grants from Society for Sedimentary Geology, Geological Society of America, and American Association of Petroleum Geologists further supplemented the research funding. I must thank my advisor, Dr. Gene Rankey, for his time, guidance and instruction. I could not have completed this project without his dedication to seeing me succeed.

I'd also like to thank my committee members: Dr. Evan Franseen for his kindness, support, encouragement, and expertise; Dr. Alison Olcott-Marshall for her patience in leading me through all the organic matter lab work, interpreting and analyzing the organic matter data and results, and explaining the results to me; and Dr. Rodrigo Garza-Perez for his logistical support out in the field, with all of the field work, obtaining permits, and for generating the bathymetric maps used in this project. I'd also like to thank him for his continuous support and encouragement, and always brightening my day or lightening my mood with his humor and light-heartedness. My committee's willingness to help and answer all of my questions is very much appreciated.

Also, I'd like to thank Matthew Downen, who was my best friend from beginning to end. He always had exceptional life advice and the right things to say to cheer me up or keep me on track. His presence, support, and example of a what an exemplar graduate student should be was invaluable to me. Also, I'd like to thank Megan Bollinger whose friendship and support throughout this process was priceless to me. I'd also like to mention and thank Bethany Winkel for her steadfast support, empathy, and encouragement. My friends are so dear and were instrumental in the completion of my thesis and my heart is filled with gratitude for them.

Table of Contents

List of Figures

Introduction

Carbonate depositional systems generally are interpreted to represent deposition on one of three end-member settings: isolated platforms, rimmed shelves, and ramps. Of modern examples of these settings, isolated carbonate platforms and rimmed shelves have long been the center and focus of study. For example, the sedimentologic and geomorphic variability of Holocene isolated platforms (e.g., Bahamas - Purdy 1963; Reijmer et al., 2009; Rankey and Reeder, 2010; Belize – Gischler 1994; Maldives – Gischler 2006; Pacific Atolls – Emery et al., 1954; Tudhope et al., 1985; Rankey et al., 2011), and rimmed shelves (e.g., South Florida - Enos and Perkins, 1979; and Belize – Purdy and Gischler 2003) have been well documented. In marked contrast, the character of Holocene carbonate ramps has not been explored as extensively (important exceptions are the Yucatan Shelf - Logan, 1969, and the Arabian Gulf - Purser, 1973; Gischler and Lomando, 2006). Yet, carbonate ramps are common in the geologic record (see summary in Burchette and Wright, 1993), and these can include considerable sedimentologic variability.

Modern carbonate ramps can provide insights on processes that influence the nature and patterns of geomorphic and sedimentologic heterogeneity in ancient analogs. Understanding the varied processes, and their influences on depositional systems, provides an actualistic basis for reconstructing ancient depositional systems. To better understand the depositional dynamics of carbonate ramps, the purpose of this study is to explore the spatial variability of sediment type, size, and sorting, and how these parameters vary with geomorphic position and oceanographic processes in the nearshore on the modern carbonate ramp of the northwestern Yucatan Peninsula, Mexico. Aspects of this system may be a modern analog for ancient carbonates. For example, the plan-view geometries of the coquina beach ridges appear broadly analogous to beach ridge

coquina reservoirs in Lower Triassic strata of western Canada (e.g., Davies et al., 1997), the Cretaceous of Texas (Kerans and Loucks, 2000), and the "Coquinas Sequence" of the Cretaceous in the presalt of offshore Brazil (although that succession is lacustrine; Carvalho et al., 2000; Jahnert et al., 2012) and Angola. Similarly, fine-grained, organic-rich, biosilicious carbonate sediment of this area shares characteristics with strata deposited in nearshore settings influenced by upwelling, such as the Mississippi Lime play in northern Oklahoma and Kansas (Watney et al., 2001; Franseen, 2006).

Background: Study Area

The Yucatan Peninsula of southeast Mexico is a broad karst plain developed on Pleistocene and older carbonate strata. Siliciclastics are absent across the area and no surface drainage systems are present (Logan, 1969). The Yucatan ramp, also known as Campeche Bank, extends northward and westward from the peninsular shoreline roughly 160-300 km into the Gulf of Mexico (Fig. 1). The slope gradient of the ramp is between 0.5-1.0 m/km or 0.03-0.06° on the northern and western sides. The shelf-slope break on the northern and western margin occurs at depths between 80-280 m. Linear shorelines on the north-facing shorelines transition to the southwest into beach ridge complexes near the towns of Celestun and Isla Arena on the western peninsular flank (Fig. 2A,B); these areas are the general focus of this study. The largest beach ridge complex (near Celestun, Fig. 2B) is approximately 30 km long and several km wide. This ridge is flanked landward by a lagoon that is home to thousands of flamingoes, and is a biosphere reserve, so was not sampled. Just south of Celestun, near Isla Arena, is a smaller beach ridge complex that is about 4 km long and less than 1 km in width (Fig 2C); this region is the area of most detailed study. South of the study area, towards Campeche, the shoreline is

dominated by mangroves and "Los Petenes," a permanently flooded salt marsh complex made up of mangroves, wetlands, salt pans, natural pools and springs, and lowland jungle.

This broad, shallow, and gently dipping shelf in the Celestun and Isla Arena area is devoid of any major, continuous topographic or reef barriers to baffle wave energy, and therefore is open to waves from the west, north, and northwest and is influenced by currents generated by easterly trade winds (Logan, 1969). The most frequent offshore wave direction is from the NE, predominantly driven by easterly trade winds (Fig. 3). With respect to the easterly trade winds, however, the northwestern Yucatan peninsula represents the "leeward" side of the peninsula. Mean annual significant wave height (H_s) offshore in this region is ~2.5 m (Appendini et al., 2012), and less nearshore, but waves vary seasonally. Between November and March, strong winds associated with northern cold fronts ("Nortes") result in large waves (H_s >2.5 m) from the N/NW (Fig. 3). The net result of the day-to-day easterly trade winds and the waves caused by the northern cold fronts is a net westward and southward offshore current on the northwestern side of the Yucatan Peninsula. The tidal regime is mixed, with a diurnal dominance, and tides range from 0.1 m (neap) to 0.8 m (spring) (Cuevas-Jimenez and Euan-Avila, 2009).

The climate of the northwestern Yucatan peninsula is tropical, with the annual air temperature ranging from 18 to 35 °C. Mean surface water temperatures on the Yucatan shelf range from 29-30°C during the summer and drop as low as 24°C in the winter, and salinity is 35-36.25 ppt (Logan, 1969). The Yucatan current, which originates off the eastern flank of the Yucatan shelf, and travels from east to west, carries upwelled, colder (16-20°C), nutrient-rich water. These upwelled waters travel west along the northern Yucatan coast, and follow the shore south along the western coast (Fig. 4) (Cochrane, 1969; Ruiz-Renteria, 1979; Merino, 1997; Zavala-Hidalgo et al., 2006; Cuevas-Jimenez and Euan-Avila, 2009; Enriquez et al., 2010;

Salmeron-Garcia et al., 2011). Merino (1997) described upwelled waters with high dissolved oxygen concentrations (3.4 - 3.7 ml/1) and a high content of nitrates, phosphates, and silicates. These elevated nutrient levels lead to a high fertilizing potential (Merino 1997), and can influence the biota and type of sediment on the western Yucatan shelf.

Methods

QuickBird remote-sensing data reveal a diversity of nearshore geomorphic elements on the northwestern Yucatan ramp, including supratidal mangrove swamp and marsh ("Petenes"), lagoon, beach ridges, and shoreface (Fig. 2C). Remote-sensing data provided a spatial context to plan the sampling strategy, choose transect locations, and determine the appropriate sampling intervals to capture the range of variability.

Two hundred and forty-two surface sediment samples across the area include seven transects with a sampling interval of 100 m. Samples were collected using small plastic vials (74 ml) which were capped at depth to preserve any fines (e.g., mud) present in the sample at the time of collection. At each sample location, a GPS point was taken with a hand-held GPS to mark the location (positional error estimated at less than two pixels on the multispectral remote-sensing data, or ~5 m), water depth was measured, sediment was collected, and bottom type was observed and recorded. Bottom type descriptions included a qualitative estimation and description of the sedimentologic and ecologic aspects at each location (e.g., benthic organisms, abundance and type of burrowing organisms, and physical sedimentary structures) to provide context for the samples and document the variability. Fifty-eight out of the 242 surface sediment samples utilized 16-ounce combusted glass jars, to avoid contamination for organic matter characterization using gas chromatography and mass spectrometry (GCMS) analysis. To further characterize ecologic trends, molluscs were collected and sieved in the field at 23 roughly evenly

spaced sampling locations on a transect across lagoon and shallow shoreface settings. In addition to the surficial sediment samples, 10 shallow (<1 m) push cores illustrate the upper parts of the Holocene sedimentary succession in a spectrum of settings. The sedimentology, fauna, and sedimentary structures in the cores were photographed and described.

Grain size, type, sorting, and origin of mud

To quantify grain sizes, granulometric analyses on the surface sediment samples used an ATM Sonic Sifter to sieve each sample. GRADISTAT software (Blott and Pye, 2001) calculated particle size statistics for each sample. Metrics include median grain size and sorting as defined by Folk and Ward (1957), with lower ϕ values indicating better sediment sorting. "Mud," as used herein, represents sediment <62.5 μm (silt and clay of the Udden-Wentworth scale). To qualitatively document grain type and sorting, ~100 representative thin sections of unsorted sediment from illustrative samples from within and among the lagoon, beach ridges, and shoreface settings were analyzed under a petrographic microscope. Thin sections represent the range of variability in sedimentology, bottom type, and geomorphology. In this manuscript, although these are sediment, not rocks, sediment is described in terms of equivalent "Dunham" textures for direct comparison with geologic analogs. Sediment "Dunham" textures were described initially in the field, but were supplemented with quantitative granulometric data and petrographic observations, and revised as appropriate.

To quantify organic matter abundance, Total Organic Carbon (TOC) measurements were taken from each of the 58 samples collected in glass jars. Additionally, several samples from the shallow cores provide information on potential stratigraphic trends. Organic matter characterization is described in the appendix.

To characterize the mud-sized fraction (< 62.5μm), two methods were used. First, 22 representative samples of all geomorphic elements were analyzed using X-ray diffraction (XRD), to determine the bulk mineralogical composition of the mud-sized fraction. Second, scanning electron microscopy (SEM; Versa 3D Dual Beam from FEI) was used to examine and identify constituents of the mud-sized fraction.

All field and laboratory observations and data were integrated using ArcGIS. Plotting data spatially enabled evaluating geomorphologic and sedimentologic trends within and among the lagoon, foreshore, and shoreface geomorphic elements.

Results

Geomorphology of Nearshore Areas

Bordered on the east by the Yucatan Peninsula, the study focus region extends west to approximately 8 km offshore, in the area near Isla Arena. Water depth ranges from 0 to ~4 m, gradually increasing westward as the distance from the foreshore increases. The shorelines at Isla Arena and just north of the study focus area (at Celestun, Fig. 2B,C) are characterized by barrier island systems that protect low-energy, mud-dominated lagoons. The coast south of the Isla Arena study area transitions into a mangrove-dominated shoreline.

Although the lagoon-barrier island-shoreface system near Isla Arena was the area of detailed sediment sampling, the patterns and geomorphic elements at Isla Arena are broadly comparable to the larger-scale system to the north. At the village of Celestun, north of Isla Arena, lies a larger (~30 km long, up to 3 km wide), and better-developed barrier island beach ridge complex (Fig. 5). These beach ridges are composed almost exclusively of coarse carbonate sediment (molluscan coquina), although salt accumulates (and is mined locally) in some lows between ridges.

The Celestun complex as a whole consists of sets of individual beach ridges. These beach ridges include spits which document recurring progradation alongshore (southward) and oceanward (west). Remote-sensing analysis (e.g., Fig. 5) suggests that the largest, first-order beach ridges (recognized by merging of smaller sets) range from 3-30 km long (average 13 km). To the north, these beach ridges include a broadly linear trend, but curve landward (to the south/southeast) at a 5-10 degree angle near their southern end. Second-order spits (that merge into the first-order beach ridges) are shorter and range in length from 0.10 to 6 km (average 1 km). These ridges also build south and terminate to the southeast, but include slightly higher angles of curvature (about 20-50 degrees) (Fig. 5).

These beach ridge complexes have changed through time. Insight into their growth patterns and rates of accumulation is evident in comparing an image of the barrier island coastline and beach ridges near Celestun from 1978 to a 2011 image of the same coastline. Comparison reveals net southward progradation of terminal beach ridges of up to 1 km in 33 years (an average of ~30 m/yr) (Fig. 6), and net shoreline accretion of up to 200 m.

Isla Arena (Fig. 2C), the focus area of sediment sampling, is located south of the Celestun complex. Isla Arena forms an elongate barrier island spit characterized by southward-diverging beach ridges, with geometries and sediment not unlike the Celestun area, except that they are an order of magnitude smaller. East of the barrier island, a protected, muddy, organic-rich lagoon (~ 4 km^2) is enclosed to the east, north, and west, but open to the open marine Gulf of Mexico to the south. Surrounding the lagoon is a dense mangrove swamp which passes into "Los Petenes," to the east.

Bathymetry, Bottom Types, and Sedimentology

The bathymetry, bottom types, sedimentology, and faunal assemblages vary markedly across the Isla Arena area. Here, geomorphic elements range from mangrove swamp and fringe, intertidal to subtidal lagoon, a north-south trending subtidal channel within the lagoon, a barrier island/foreshore system, and shoreface, and reflect bathymetric variability. Remote sensing data was integrated with the 242 bathymetric field measurements to generate a bathymetry map of the study area (Fig. 7). Each of these elements include distinct bottom type, sedimentologic character, biota, and TOC (Fig. 8).

In the study area, the landwardmost area, "Los Petenes," is a permanently flooded marsh with a diversity of habitats (including mangrove marsh, wetlands, salt pans, lowland jungle, and natural freshwater pools and springs) that extends approximately 10 km inland (eastward) from the lagoon near Isla Arena to outcropping bedrock. White mangroves (*Laguncularia racemosa*) mixed with freshwater grasses and sedges occur furthest inland (Fig. 9A; this area was not surveyed to any extent) and transition westward into a swampy, black mangrove (*Avicennia germinans*)-dominated zone that spans approximately 0.2 km to 3.5 km inland from the eastern coast (Fig. 9B). The sediment in this black mangrove zone is tan mudstone to fine wackestone with microbial mats and desiccation features at the surface. Mangrove roots and woody fragments, in addition to gastropods and bivalves, are common (Fig. 9C). Black mangroves transition to the red mangroves (*Rhizophora mangle*) that fringe the lagoon (Fig. 9D). Along the mangrove-rich flanks of the lagoon, sediment texture ranges from wackestone to packstone (Fig. 9E). This sediment consists of very poorly sorted coarse to fine sand and gravel with a minor mud and silt fraction (mean grain size of 618 μm; N = 5) (Fig. 8B-D). The dominant grains are bivalves and gastropods, some of which are whole and are identifiable to species level. Barnacles

(such as *Amphibalanus improvises*) are prolific. and the mangrove root-encrusting oyster, *Crassostrea rhizophorae*, is also present. The mangrove fringe is the most organic matter-rich geomorphic element in the study area (TOC = ~15%) (Fig. 8F,9F).

Flanking the mangrove fringe is the intertidal to shallow subtidal protected lagoon, in which water depths are less than 2 m. The lagoon has a fairly consistent depth trend – shallower near the mangrove fringe and up-dip (N) within the lagoon, and deeper towards the center (e.g., N-S trending tidal channel) and to the south, towards the open ocean. The greatest water depths (up to 2 m) are found in the north - south trending tidal channel that runs down the middle of the lagoon (Fig. 7, 8A). Much of the bottom is covered by *Syringodium filiforme*, *Halodule wrightii*, and *Thalassia testudinum* (Fig. 9G). The dominant grains are bivalves and gastropods, but miliolid foraminifera are present throughout the lagoon (<10%, mostly <5%, by abundance), in addition to some peneropolid foraminifera. The northern, and most restricted, part of the lagoon is dominated by mudstone to wackestone, and the sediment consists of very poorly sorted mud to fine sand (mean grain size of 213 μm; N = 11). To the south, in the more open lagoon, sediment texture transitions to slightly coarser and grainier wackestone (mean grain size of 345 μm; N= 18) (Fig. 8B). The intertidal to shallow subtidal lagoon as a whole is mud dominated (many samples have >20% mud), with exception of the N-S trending tidal channel, which is dominated by molluscan coarse sand and gravel (mean grain size of 2738 μm; N = 7) (Fig. 8C-D, 9H). Total Organic Carbon (TOC) is elevated in the lagoon (up to 15%; Fig. 8F), with increased organic matter content near the mangrove fringe. In core, sediment from the lagoon varies from mudstone to packstone and rare mud-lean packstone, with whole or slightly disarticulated shells (Figure 10A-C).

West of the lagoon, the barrier island spit of Isla Arena consists of molluscan coquina beach ridges that have extended 3.5 km southward, but reach less than 300 m across (Fig. 2C). The beach ridges are dominated by whole and fragmented bivalve and gastropod shells. Sediment is composed of gravel to coarse sand with no mud (mean grain size of 4111 μm; N = 3) (Fig. 8C-E). The beach ridges include trough and planar-tabular cross-bedding, and coarse (gravel) to fine (sand and gravel) layering that is horizontal to gently seaward dipping (Fig. 11A-B).

Directly south of the barrier island spit, a subtidal bathymetric high continues to the south. This high is flanked to the east by an area that is slightly deeper (1.5-2 m), and includes a few channels that cut across the bar (Fig. 7A, 8A). In these areas, the sediment on the bathymetric highs is coarse sand to gravel (mean grain size of 1957 μm; N = 19) and the texture is packstone to grainstone; most grains are broken and abraided (Fig. 10D). Landward (eastward) of this bathymetric high, the *Thalassia*-covered subtidal bottom (up to 2 m deep) has an increased proportion of fines and mud (mean grain size of 696 μm; N = 14; mud ranges to in excess of 20%), and the sediment texture is primarily wackestone to packstone, although locally, coarse grain-dominated packstone is present near the mangrove fringe (mean grain size of 1805 μm; N = 5). This change in texture and grain size is related to the greater abundance of bivalves, gastropods, barnacles, and oysters in the sediment and on the mangrove prop roots. Bivalves and gastropods are the most abundant macrofauna and sediment constituents across this area, but foraminifera occur widely as well.

Sediment in fully open marine areas offshore of Isla Arena and the bar south of Isla Arena differs in texture and composition, and some changes follow shore-parallel belts. Just offshore (west, <1 km) of Isla Arena, sediment texture ranges from wackestone to (more

commonly) packstone (Fig. 8B). It consists of sand to gravel (average grain size 2086 μm; N = 27) with the exception of sea grass patches (Fig. 11C) that are scattered intermittently throughout the offshore, in which the proportion of mud and fine sediment increases (Fig. 8E). A second zone occurs further offshore (1-3 km from Isla Arena), as water depth gradually increases (up to ~3 meters deep, 3 km offshore of Isla Arena). In these areas with common sea grass cover, the proportion of mud and fine grains increases (mud abundance between 5-20%), as the proportion of coarse grains decreases, and medium-size grains remains constant (the average grain size is 767 μm; N = 13) (Fig. 8E). The dominant Dunham textures in this area are wackestone to packstone. Another transition occurs roughly 3 km offshore, where *Halimeda* is the dominant sediment type with large bushes of the green algae (Fig. 11D-E). Sediment texture is grainstone and is composed mostly of gravel with common sand-sized fraction (average grain size of 2322 μm; N = 9) (Fig. 8E,11F). Miliolid foraminifera are present throughout the shoreface, in addition to planktonic forams, but molluscs and *Halimeda* are the dominant sediment producers and constituents. Maximum water depth measured 8 km offshore, at the furthest offshore extent of the study area, is 4 meters. TOC values across the offshore areas are less than 2% (Fig. 8F).

A distinctive assemblage of molluscs is evident between the lagoon (including the mangrove fringe) and offshore. In total, the lagoon includes different species and greater diversity than the assemblage of molluscs offshore. In detail, the lagoonal assemblage includes the bivalves *Chione cancellata* (Fig. 12A), *Cardita floridana* (Fig. 12B), *Anomalocardia auberiana* (Fig. 12C), *Tellina alternata* (Fig. 12D) and a very distinctive, white, oval to rectangular bivalve, *Tagelus plebius*, which is known to inhabit mud-dominated sediment (Fig. 12G); the barnacle *Amphibalanus improvisus* (Fig. 12E); the gastropod, *Bulla occidentalis* (Fig. 12F), and an abundance of high-spired gastropods of the genus *Cerithium* (Fig. 12H).

Crassostrea rhizophorae (Fig. 12I), an oyster that attaches to the roots of red mangroves, is also part of the lagoonal assemblage. *Melongena bispinosa* (Fig. 12K) is common near the mangrove fringe, as are several different types of intensely bored or otherwise unidentified gastropods (Fig. 12K).

In general, although the lagoonal molluscan assemblage is evident in the area south of the lagoon but behind the bathymetric ridge (Fig. 7), some distinctions are present. For example, the clam, *Mercenaria mercenaria*, which is larger than the species of bivalves found within the lagoon, inhabits the subtidal area south of the lagoon. Like many of the coarser grains in this area, these large clams are encrusted with serpulid worm tubes and the barnacle, *Amphibalanus improvisus*, in addition to being heavily bored by the red boring sponge, *Clionidae* (Fig. 12L, M).

The shoreface sediment is dominated by bivalves, most commonly and abundantly by the species *Chione cancellata* (Fig. 12A), *Cardita floridana* (Fig. 12B), *Anomalocardia auberiana* (Fig. 12C), and *Tellina alternata* (Fig. 12D). *Busycon coarctatum*, a larger gastropod (Fig. 12N), and the bivalve *Dinocardium robustum* (Fig. 12O) also inhabit the offshore.

Character of the Fine Fraction

Previous studies of the fine fraction (< 63μm) of carbonate-dominated successions have suggested a diversity of mineralogy, reflecting distinct sources (e.g. see Gischler et al., 2013 and O'Connell and James, 2015 for summaries). Given the abundance of mud in the study area on the western side of the Yucatan Peninsula, the nature and composition of the carbonate mud and fine fraction of the sediment was examined. Scanning electron microscopy (SEM) and X-ray diffraction (XRD) provide tools to explore the mud-sized sediment composition and if it varies spatially.

SEM observations of the mud-sized portion illustrate a diversity of particles (Fig. 13). The majority of the sediment is made of non-descript carbonate particles (Fig. 13A). The presence of some microstructure in parts of these particles suggests that they may be amalgamations of highly abraded skeletal fragments that have flocculated together to form small (~10-50 µm) clumps of carbonate mud.

XRD estimates of the bulk mineralogy of the carbonate mud suggest a dominance of calcite. Relative abundance of calcite within the lagoon is largely consistent, ranging mostly between 64 - 72% (average = 68%), as aragonite ranges from 28-36% (average = 32%). Relative abundance of calcite in the shoreface includes a wider range and has overall a slightly lower abundance of calcite than in the lagoon. Calcite abundance in the shoreface ranges from 37.5-75% (average = 62%), and aragonite ranges from 25-62.5% (average = 38%).

Beyond these non-discript carbonate grains, an interesting finding was the abundance and widespread presence of biosilicious particles, including siliceous diatoms and sponge spicules (Fig. 13A-I). The most common type of diatom occurs as isolated wheel-shaped particles ~30 µm in diameter or as rods that can exceed 125 µm in length (e.g., Fig. 13A,B), that appear to be chains of the wheel-shaped particles. Sponge spicules include rod-shaped particles, as well as other, more complex morphologies (Fig. 13G,I). Other identifiable particles in the fine fraction include dinoflagellate spores (Fig. 13J-L), coccolithophores (Fig. 13M), echinoid spines (Fig. 13N), clionid-sponge borings (Fig. 13O), and tunicate spicules.

Visual SEM observations of these fine-fraction constituent particles from an illustrative transect of 22 samples extending from the landward side of the lagoon to 8 km offshore reveals that the distribution and abundance of particles is relatively uniform and consistent across the area. The nondescript carbonate particles are present throughout the lagoon and shoreface areas,

as are the diatoms and sponge spicules, with no obvious changes in relative abundance of the different types of particles. The only clear distinction between the lagoon and shoreface is that the diatoms in the offshore are longer than the diatoms in the lagoon (e.g., they include more stacked "wheels").

Discussion

Controls on Sedimentology and Geomorphology

The geomorphology and sedimentology of this Holocene carbonate ramp system illustrate considerable variability. From a nearshore marsh ("Petenes"), to muddy lagoons, coquina-rich barrier 'islets', and to the shoreface, the water depths, bottom types, and sediment vary considerably. This variability is interpreted to be influenced by physical, chemical, and biological oceanographic processes.

In terms of physical oceanographic processes, currents generated by the day-to-day easterly trade winds and by larger waves caused by the northern cold fronts, which occur generally between November through March, have the net effect of transporting sediment southward along the northwestern Yucatan Peninsula (Appendini et al., 2012). Offshore, in water greater than ~2 m depth, subaqueous dunes or widespread current ripples are rare, suggesting that the bedload portion may not be markedly transported alongshore. Nearshore, in the uppermost shoreface to foreshore areas with the most intense wave and current activity, sediment accretion forms the beach ridges, features which build southward and step oceanward (westward) as each successive beach ridge builds out over the previous ridge (Fig. 5). Collectively, the accretion pattern of the beach ridges reveals that both barrier island spits (Isla

Arena and Celestun) have prograded southward and westward in sets of beach ridges in a repeated and predictable pattern (Fig. 5).

The barrier island spits at Celestun and Isla Arena in turn act as a barrier to the offshore wind and wave energy, creating semi-restricted, lower-energy lagoons in their lee. In these lagoons, finer sediment (including abundant mud and fines) and organic matter settles and accumulates. The lagoon is hydrodynamically connected with the open ocean, sufficient for sediment from the open ocean to be transported into the lagoon, as indicated by the abundance of diatoms, sponge spicules and mixed organic matter types (both plant and algal; see Appendix 1). Yet, conditions are distinct, as evidenced by the differences in mud abundance, and the varied *in situ* carbonate production, as indicated by the segregated molluscan faunal associations and common miliolines in the lagoon. The dominant foraminifera, miliolines (alveolinids, soritids, peneroplids, and miliolids), generally tolerate higher salinities (Hallock and Glenn, 1986), and so can become dominant in more restricted or variable-salinity settings. Also, Hallock and Glenn (1986) indicate that miliolids, peneroplids, and small rotaliine are most common in quiet-water settings that accumulate fine sediment, like the Isla Arena lagoon.

In addition to physical processes, chemical oceanographic factors likely influence the sediment of the area. Upwelled cool waters (~17-18°C) with elevated nutrient levels are transported westward seasonally along the northern Yucatan coast, tracking southward along the northwestern coast (Fig. 4). In some cases, these upwelled waters of the northern and western Yucatan ramp include chlorophyll levels that can reach in excess of 5 mg/m^3, and thus the area is subject to eutrophic to hypertrophic conditions. These elevated levels contrast markedly with typical open-marine, tropical to subtropical waters, which include chlorophyll between 0.01 and 0.1 mg/m^3. Elevated nutrient levels could be reflected in the sediment in several ways. First,

nutrient-rich carbonate systems commonly are associated with the heterozoan carbonate association (James, 1997; Mutti and Hallock, 2003). The paucity of corals and coral reefs in the region may reflect this factor, as corals prefer oligotrophic environments in which chlorophyll levels are low. Similarly, the dominance of carbonate-producing biota of the heterozoan association (benthic foraminifers, bivalves, gastropods, echinoderms, barnacles, and bryozoans) is consistent with the presence and influence of cooler, nutrient-rich upwelled waters in the region. Beyond carbonate sediment, nutrient supply increases the occurrence and relative abundance of sponges, and plankton biomass. This primary production and elevated nutrients likewise lead to the presence of biosilicious organisms (e.g., diatoms), dinoflagellate spores, and coccolithophores (Mutti and Hallock, 2003). In addition to upwelling, another potential source of nutrients on the northwestern Yucatan Peninsula is freshwater springs and groundwater discharge into the lagoons and coastal waters. The trophic index for silica at Celestun, is eutropic due to the input by groundwater springs and natural runoff (Herrera-Silveira et al., 2002), and freshwater springs are present in the shallow marine areas south of Isla Arena as well.

At first glance, the presence of *Halimeda*, a photosynthetic green algae, may seem more aligned with the photozoan association. Although *Halimeda* is common in Holocene photozoan systems (James, 1997), the genera can occur (and be abundant) in areas with elevated nutrients (Marshall and Davies, 1988). *Halimeda* growth responds to, and can be favored by, nutrient-rich water, and therefore is not inconsistent with the presence of at least episodically elevated nutrients. In fact, shallow species of *Halimeda* are adapted to take advantage of episodic nutrient pulses (Littler et al., 1988).

Contrasts with other Holocene Systems

The processes, sediment and geomorphology of this Yucatan region contrast with other well-studied carbonate areas. For example, another well-studied Holocene carbonate ramp occurs in the southern Arabian Gulf, in the United Arab Emirates (UAE). In distinction to the Yucatan region, the UAE includes an arid, subtropical climate, which favors the deposition of evaporites, sabkhas (arid tidal flats), and eolianites. Nearshore processes in this area are impacted by large, on-shore waves caused by the strong, northeasterly ("shamal") winds and by large tidal amplitude (~2 m) in the open Arabian Gulf. These factors, in addition to the restriction and supersaturation created by the islands and tidal deltas and inlets, create an environment conducive to the formation of ooids, peloids, and aggregate grains. At the southern end of the Arabian Gulf, the coastline includes offshore subtidal reefs and cemented hardgrounds, and oolitic tidal deltas between islands (Purser, 1973). Lagoons are protected from open ocean conditions by the deltas and islands, and include subtidal to intertidal foraminifera- and gastropod-rich sediment, flanked landward by sabkhas with microbial mats, desiccation cracks, and evaporite minerals (Kendall and Skipwith, 1969).

One commonality between the southern Arabian Gulf and the northwestern Yucatan is the presence of beach ridges composed of medium to coarse grained skeletal fragments, including abundant gastropods. However, the beach ridges in the Arabian Gulf also contain quartz sand, which those on the northwestern Yucatan do not, and are reworked into eolian dunes by the strong shamal winds. Similarly, although there are small, scattered salt pans between beach ridges near Celestun on the northwestern Yucatan coast, they are not on the same scale or as widespread and as well-developed as the evaporitic supratidal sabkhas in the Arabian Gulf. These sabkhas reach up to about 8 km wide and extend for hundreds of kms along strike (NE-

SW) (Rankey and Berkeley, 2011). Instead of the sabkhas, because of the tropical and more humid climate, the supratidal region of the northwestern Yucatan is made up of a permanently flooded salt marsh made up of mangroves, lowland jungle, and wetlands. Another sedimentologic difference is the presence of ooids and peloids in the Arabian Gulf, which are absent in the northwestern Yucatan. The presence of these grains in the Arabian Gulf is likely related to the elevated tidal current speeds and supersaturated waters.

Comparing the Yucatan to another well-studied Holocene carbonate system, the Florida Shelf includes geomorphic forms and sediment distinct from the northwest Yucatan area, even beyond the self-evident difference of ramp versus rimmed shelf (e.g., Ginsburg, 1956; Enos, 1977). At the largest scale, the Yucatan ramp does not have a reef that baffles wave energy like the linear reef tract at the Florida shelf margin. The Pleistocene bedrock highs of the Florida Keys form the dominant restriction-causing element. In the Yucatan, the barrier islands at Isla Arena and Celestun serve as topographic barriers that create lower-energy, more restricted lagoon environments in their lee. Geomorphically, Florida Bay ("inner shelf") includes reticulate intertidal to supratidal mud banks up to several 100 m across, separated by subtidal areas ("lakes") several meters deep and up to several km across (Enos, 1989). In contrast, the intertidal to shallow subtidal lagoons at Isla Arena and Celestun have fairly consistent depth trends, shallower near the mangrove fringes and updip within the lagoons (Fig. 7). They increase in depth toward the center of the lagoons (e.g., the axial channels), and to the south, toward the open ocean.

These Yucatan lagoons include several sedimentologic similarities with Florida Bay, however. Both Florida Bay and the Yucatan lagoons have a high proportion of fine sand- and mud-sized sediment (in many cases, more than 50%), and molluscs and foraminifera are the

dominant fauna. Whereas the Florida inner shelf and Yucatan lagoons have sedimentologic and faunal similarities, the wholly subtidal, open marine Florida shelf differs from the barrier islands and offshore of the Yucatan ramp. Although both the Florida shelf margin and offshore Yucatan have coarser grains than the nearby protected (lower-energy and more restricted) areas, they have distinct grain associations. The common coral fragments in the sediment of the Florida shelf reflect the abundance of coral reefs, whereas corals are rare on the northwestern Yucatan shelf. *Halimeda*, an important contributor in the Florida outer shelf, commonly is interpreted to be sourced from the reefs (Enos, 1977). Although it includes no reefs, *Halimeda* is a dominant sediment contributor in the offshore region in the Yucatan study area, most abundant in water depths of 2+ m, where it grows directly on the seafloor (Fig. 11), rather than in reefs. Bivalves are a much more common and abundant carbonate sediment contributor in the Yucatan field area. A key difference between the two areas is the high abundance of siliceous diatoms and sponge spicules on the northwestern Yucatan, and the scarcity of those constituents on the Florida shelf.

These contrasts are interpreted to be related to differences in environmental conditions. The Florida shelf margin faces the dominant easterlies, and the Pleistocene bedrock has formed a rigid energy baffle that protects Florida Bay. In contrast, the Yucatan shelf focus area is on the leeward margin of the Peninsula, protected from the easterly trade winds, but facing directly into waves generated by winter cold fronts from the north ("Nortes"). Currents generated by the Nortes and the Yucatan current cause a net southward transport (of nutrients and sediment) along the northwestern coast of the Yucatan. These factors are interpreted to control the growth of the barrier islands and consequent formation of the lagoons. Additionally, the elevated nutrients influence the biota, driving the heterozoan association and the presence of siliceous organisms.

The sediment of the northwestern Yucatan also contrasts with sediment found on the shallow carbonate platforms of the Bahamas. Bahamian platforms include ubiquitous non-skeletal sand (peloids, ooids, etc) and abundant mud (Purdy, 1963; Reijmer et al., 2008; Rankey and Reeder, 2010). The aragonite mud in the Bahamas commonly is interpreted to be physio-chemically precipitated from highly supersaturated water of elevated salinity. For example, Milliman (1993), Gischler et al. (2001), and Gischler et al. (2013) showed that mud from the Bahamas has high aragonite content, with elevated strontium concentrations, and, suggested physio-chemical precipitation as the dominant mechanism by which mud is produced. Similarly, Rankey and Reeder (2010) and Rankey (2014) argued that the elevated carbonate supersaturation state of Bahamian waters also favored the production of ooids and preservation of peloids, even on "low energy" leeward margins and shorefaces.

In sharp contrast, no ooids or peloids are evident in the northwestern Yucatan Holocene sediment. And, in comparison with the Bahamian mud fraction, Yucatan mud is more dominantly calcite with some biosilicious material (Fig. 13). The mud on the northwestern Yucatan shelf is composed mainly of non-descript calcareous aggregate particles, derived from mollusc fragments, foraminifera, *Halimeda,* echinoids, and barnacles, but also includes a notable contribution from sponge spicules, diatoms, and tunicate spicules. Coccolithophores and dinoflagellates also make up a minor component of the mud-sized fraction. Bahamian mud includes a pronounced contribution from fine aragonite needles (e.g., Milliman et al., 1993) These differences are interpreted to reflect the convergence of several factors. First, the lower carbonate saturation state and cooler temperatures may inhibit the physio-chemical precipitation of mud (e.g., whitings), compared to the Bahamas. Second, the upwelled, cooler waters, which introduce elevated nutrients into the system, favor the proliferation of biosilicious and

heterozoan organisms, resulting in sediment dominated by calcite and silica composition. The mud fraction may come from local bioerosion (Matthews, 1966), transported in from offshore, transported in from higher-energy north coast (Appendini et al., 2012), or *in situ* production.

The data from this Holocene ramp provide an actualistic conceptual model for the nature of low-energy carbonate ramp systems (Fig. 14A,B). The results emphasize several important controls that may be underappreciated or that have not been widely interpreted in the stratigraphic record. One example is the role of upwelling in introducing cooler, nutrient-rich waters into tropical systems (Fig. 14A) (cf. Westphal et al., 2010). These upwelled waters markedly impact the assemblage of sediment-producing organisms. Whereas many biosiliceous or heterozoan carbonate successions have been interpreted as high-latitude, deep basinal or cool- to cold-water settings, the northwest Yucatan provides a modern example that illustrates that upwelling can favor a shallow, nearshore, tropical environment that includes biosiliceous sediment, ubiquitous heterozoan-assemblage carbonate producers, but is mostly devoid of corals and reefs.

Beyond upwelling, the western Yucatan coast is a low-energy, leeward coastline (with respect to the easterly trade winds) for the majority of the year (Fig 14A). In this setting, fine carbonate sediment and mud, some of which is sourced by plankton blooms from cooler upwelled water (Fig. 4A-C) can be ubiquitous. These blooms create turbid, muddy conditions in the nutrient-rich water, a suboptimal condition for reefs and corals. Ultimately, however, the mud settles and accumulates in lower-energy settings.

The area is impacted by winter cold fronts, which appear to drive the accumulation of the beach ridge complexes (Fig. 14B). The shoreline orientation relative to the approach of offshore

"Norte" waves, coupled with the west- and south-moving regional current, drives southward longshore transport and growth of beach ridges (Figs. 5, 14B).

The geomorphology and sedimentology of the northwest Yucatan shelf therefore is interpreted to reflect a distinct combination of several factors: pre-existing gradient, the leeward setting, an alongshore current that sporadically carries upwelled cooler, nutrient-rich waters, and winter cold fronts. These factors, in concert with one another, ultimately determine the sediment composition and facies that form (e.g., Fig. 15), and could be recorded in the rock record.

Comparison with Ancient Carbonate Ramps

The results of this study illustrate physical (energy level, SST) and chemical (upwelled waters) oceanographic influences on the geomorphology and sedimentology of a Holocene ramp system. Although many ancient successions containing biosiliceous sediment and heterozoan carbonates were interpreted to have been deposited in deep basinal or cool- to cold-water settings, recent interpretations and studies have suggested that these deposits can occur in tropical to subtropical settings in which elevated nutrient levels and upwelling are present (see Westpahl et al. 2010 for a summary). The Yucatan ramp serves as a modern example of such an instance and can be compared to other ancient ramp systems in which upwelling and elevated nutrient levels could have contributed to an abundance of biosiliceous sediment and the dominance of heterozoan carbonates.

In one well-documented example, Mississippian (Osagean) strata in central Kansas (Franseen, 2006) represent deposition on a sub-tropical/tropical, shallow marine, inner-ramp setting. These strata consist of cherty biosiliceous and heterozoan carbonate facies and form reservoirs in central Kansas, with cumulative production of more than 1 billion barrels (Franseen, 2006; Adkins-Heljeson et al.,1999). Much like the sediment on the nearshore

northwestern Yucatan ramp, the Osagean strata of central Kansas are rich in siliceous sponge spicules, echinoderms, bryozoans, gastropods, brachiopods, and ostrocods. The interpreted depositional environment and associated depositional model and geomorphic elements for the Osagean (Franseen 2006) is broadly similar to the modern nearshore environment and geomorphic elements on the northwestern Yucatan peninsula. The skeletal grainstone and packstone were likely shoals or some type of topographic barrier, which created a semi-restricted lagoon or embayment on their leeward flank. These interpreted protected areas are the sites for deposition of fine-grained (mudstone to wackestone) facies. These characteristics, in general terms, may be similar to the coquina-rich barrier island-lagoon systems at Isla Arena and Celestun, although the Mississippian covers a much larger area (10s-100s of km).

The Mississippian paleogeographic setting for the midcontinent was in the low latitudes; Kansas was at ~20° south latitude during the Osagean. Paleogeographic reconstructions of the area (Gutschick and Sandberg, 1983) and consideration of predicted wind circulation patterns and orientations of basins led Parrish et al., 1983 to suggest coastal upwelling as the process responsible for abundant chert (siliceous sponges) on the margins of basins. Franseen, 2006 interpreted that the upwelling affected inner ramp areas adjacent to the Anadarko Basin, resulting in the dominance of heterozoan and biosiliceous facies, and absence of photozoans. Like on the Holocene Yucatan shelf, these upwelled waters may have suppressed photozoan carbonate sediment production and created an environment where heterozoan carbonate producers and siliceous sponges flourished, even in the shallow marine, low-latitude setting (Franseen 2006).

Another well-studied example of an ancient ramp system is the Permian San Andres and Grayburg formations of the Permian Basin in west Texas. Specifically, these strata were deposited on a distally steepened ramp setting, broadly comparable in some ways to the

northwestern Yucatan ramp. The strata suggest deposition in settings from inner ramp (evaporites, siliciclastics, and muddy carbonates, reflecting updip-most marine influence), middle ramp (muddy and peloidal carbonates, interpreted to be lagoonal), ramp crest (ooid, peloid, and skeletal grainstone, representing high-energy shoals), to outer ramp (mud-bearing skeletal sediment deposited in offshore, low energy settings) (Kerans and Fitchen, 1995).

The shallow-water deposits of the San Andres and Grayburg formations include similarities and differences with modern sediment of the Yucatan shelf. In updip-most strata, carbonate mudstone is associated with tepee-pisolite-fenestral and algal-laminated facies, implying a restricted shallow subtidal to peritidal environment (Barnaby and Ward 2007). These sediments are broadly comparable to the mud-dominated, algal laminated sediment of the Petenes on the northwestern Yucatan (e.g., Fig. 9C). Early cementation, teepees, pisoids, and evaporite (sabkha) deposits, however, were not recognized near Isla Arena. These differences may be related to a more arid Permian climate, a setting that would have contributed to the formation of dessication cracks and evaporites. This situation contrasts to the semi-arid tropical climate of the northwestern Yucatan, which is not conducive to widespread and well-developed bedded evaporites, although thin evaporites do occur.

The peloid and ooid grainstones of the San Andres-Grayburg interval commonly are interpreted to record high-energy conditions and shallow-water deposition on the ramp crest. These strata are interpreted variably as a wave-dominated setting (although a shoreface and foreshore was not described; Ruppel and Ward, 2013) or tidally influenced setting (with bars and channels; Barnaby and Ward, 2007). In contrast, the northwestern Yucatan has no depositional ramp crest, in the sense used in these Permian strata (either tidal or wave-dominated), but rather the shoreface dips gently outboard from the foreshore and beach ridges of the barrier islands of

Celestun and Isla Arena. These distinctions therefore appear to be due to different hydrodynamic conditions.

Other differences include the presence of high-energy ooid and peloid packstone to grainstone, sediment types which are absent on the northwestern Yucatan shelf. Carbonate-supersaturated waters and high energy (tidal or wave) conditions favor these sediment accumulations (e.g., Rankey and Reeder, 2010; Rankey 2014), and likely contributed to the formation of ooids and peloids (and the early cementation) in these Permian Basin strata (Barnaby and Ward 2007). In contrast, lower saturation states and unsuitable hydrodynamic conditions (Reeder and Rankey, 2008) in the northwest Yucatan may inhibit their formation and accumulation there.

Finally, parts of the Lower Triassic Montney Formation of the Western Canadian Basin include dolomitized bivalve-molluscan coquina, deposits which locally form an important reservoir. Davies et al. (1997) describe the Montney Formation as being deposited in a mid-latitude (~30N) setting, on the northwestern coast of the Pangean supercontinent in a seasonally hot and arid environment.

Factors that influenced the deposition of the Montney Formation include the dominant northeast (offshore-oriented) trade winds, offshore coastal upwelling, and north to south longshore sediment transport caused by wave and wave-generated currents with a minor tidal influence. These conditions have been interpreted (Davies et al. 1997) to lead to deposition of coquina ridges that extend up to 400 km long, are nearly continuous, and are about 30 km wide and up to 30 m thick. These general conditions (leeward position, nearby upwelling, longshore currents) and the product (molluscan coquina beach ridges) are similar to those on the northwest Yucatan.

These deposits have some differences, however. One major difference between the Montney coquina ridges and the northwestern Yucatan coquina beach ridges is that the Montney coquina ridges are associated with sandstone and siltstone, dominantly shoreface and storm-reworked (HCS) deposits and turbidite facies. It is important to note, however, that the siliciclastic deposits may not be time-equivalent with the coquina deposits (Davies et al., 1997). Unlike the beach ridges on the northewestern Yucatan, which are highstand deposits, the thickest coquina deposits represent accumulation during a forced regression and lowstand (Davies et al. 1997). Currently, during the present highstand, the coquina beach ridges on the northwestern Yucatan are prograding to the south and basinward (westward). If sea-level were to drop, the beach ridges could begin to build out and prograde basinward (westward) as the upper shoreface and foreshore stepped down and outward away from the present-day peninsular shoreline. Thus, although the scale of the two accumulations are quite different at present, the Yucatan Holocene ridges could increase in size in time.

Another divergence between the two systems is the diversity of molluscs. Davies et al. (1997) note that the Montney coquina is dominated by mainly two genera of bivalve molluscs, suggesting that the environment could have been a hypersaline or stressed environment, which would restrict the diversity of bivalves. The coquina beach ridges on the northwestern Yucatan, on the other hand, are composed of four major bivalve species, two minor bivalve and gastropod species, and occasional barnacle fragments. The faunal diversity on the northwestern Yucatan is greater than that of the Montney Formation, perhaps due to more normal marine conditions or less persistent upwelling on the northwestern Yucatan coast than during deposition of the Montney Formation.

Summary and Conclusions

This study explored links between geomorphology and sedimentology (carbonate, biosilicious, and organic matter) on shoreface-beach ridge-lagoon systems on a low-energy, Holocene carbonate ramp on the northwestern Yucatan shelf. The trends are interpreted to represent the coupled influences of physical (waves, currents, tides, SST) and chemical (nutrient levels), biological (sediment production), oceanographic processes.

In this area, subtidal shoreface regions include shore-parallel belts of *Halimeda*-rich muddy gravel and skeletal (mainly molluscan) muddy sand to gravel. Currents generated by the day-to-day easterly trade winds and by larger "Norte" waves transport sediment and upwelled waters southward along the northwestern Yucatan Peninsula. Longshore sediment transport along the coastline forms barrier islands, which consist of molluscan coquina beach ridges. The succession of these ridges have prograded southward and westward, at rates >10 m/yr. These barrier islands at Celestun and Isla Arena include semi-restricted, low-energy lagoons in their lee. These lagoons contain abundant fine sediment (including mud contents of >20%) and organic matter (up to 15%). Landward, a broad supratidal marsh (the "Petenes") includes dominantly carbonate mud, and passes gradationally into terrestrial habitats.

In addition to physical processes, chemical oceanographic factors are interpreted to influence the sedimentologic character of this ramp system. Upwelled cool (~17-18°C) waters with elevated nutrient levels are transported westward seasonally along the northern Yucatan coast, then pass southward, following the northwestern coast; freshwater springs and groundwater also may introduce nutrients into the lagoons and coastal waters. The elevated nutrients favor the dominance of heterozoan carbonate producers and the abundance of biosiliceous skeletons. Offshore sediment includes a mixed heterozoan (bivalves, gastropods,

barnacles, foraminfera, bryozoans, and sponges) and photozoan assemblage (*Halimeda*), in addition to diatoms, sponge spicules, dinoflagellates, and coccolithophores. The foreshore and beach ridges include bivalve- and gastropod-rich coquina. In the lee of the barrier island, biosiliceous, organic matter-rich, carbonate mud with common bivalves and foraminifera occurs in a shallow, protected lagoon.

In summary, the results of this study illustrate that sedimentologic, organic matter, and geomorphic variability are influenced by physical (energy level, SST) and chemical processes (upwelled waters). The insights provide a conceptual model for the nature and controls on sedimentologic and geomorphic heterogeneity on this ramp system, and may enhance understanding of ancient low-energy, fine-grained carbonate systems, some of which include prolific hydrocarbon reservoirs.

References

APPENDINI, C.M., SALLES, P., MENDOZA, T.E., LOPEZ, J., AND TORRES-FREYERMUTH, A., 2012, Longshore sediment transport on the northern coast of the Yucatan Peninsula: Journal of Coastal Research, v. 28, p. 1404 – 1417.

BARNABY, R.J., AND WARD, W.B., 2007, Outcrop analog for mixed siliciclastic–carbonate ramp reservoirs—stratigraphic hierarchy, facies architecture, and geologic heterogeneity: Grayburg Formation, Permian Basin, U.S.A.: Journal of Sedimentary Research, v. 77, p. 34–58.

BLOTT, S. J., AND PYE, K., 2001, Gradistat: A grain-size distribution and statistics package for the analysis of unconsolidated sediments: Earth Surface Processes and Landforms, v. 26, p. 1237–1248.

BURCHETTE, T.P. AND WRIGHT, V.P., 1992, Carbonate ramp depositional systems: Sedimentary Geology, v. 79, p. 3–59.

CARVALHO, M.D., PRAÇA, U.M., TELLES JR., A.C.S., JAHNERT, R.J., DIAS, J.L., 2000, Bioclastic carbonate lacustrine facies models in Campos Basin (Lower Cretaceous), Brazil. In: Gierlowski-Kordesch, E., Kelts, K.R. (Eds.), Lake Basins Through Space and Time, p. 245–255.

COCHRANE, J.D., 1969, Water and circulation on Campeche Bank in May: Papers in Dedication to Professor Michitaka Uda: Special Bulletin of the Japanese Society of Fisheries Oceanography, p. 123–129.

CUEVAS-JIMENEZ, A. AND EUAN-AVILA, J., 2009, Morphodynamics of carbonate beaches in the Yucatan Peninsula: Ciencias Marinas, v. 35, 307–320.

DAVIES, G. R., MOSLOW, T. F. AND SHERWIN, M. D. 1997, The lower Triassic Montney Formation, west-central Alberta. In: Triassic of the Western Canada Sedimentary Basin. T.F. Moslow and J. Wittenberg (eds.). Bulletin of Canadian Petroleum Geology, v. 45, p. 474–505.

EMERY, K.O., 1956, Marine geology of Johnston Island and its surrounding shallows, central Pacific Ocean: Geological Society of America Bulletin, v. 67, p. 1505–1520.

ENRIQUEZ, C., MARINO-TAPIA, I.J., AND HERRERA-SILVEIRA, J.A., 2010, Dispersion in the Yucatan coastal zone: implications for red tide events: Continental Shelf Research, v. 30, p. 127–137.

FOLK, R.L., AND WARD, W.C., 1957, Brazos river bar: a study of significance of grain size parameters: Journal of Sedimentary Petrology, v. 27, p. 3–26.

FRANSEEN, E. K., 2006, Mississippian (Osagean) Shallow-water, mid-latitude siliceous sponge spicule and heterozoan carbonate facies: An example from Kansas with implications for

regional controls and distribution of potential reservoir facies: Current research in earth sciences, Kansas Geological Survey Bulletin, v. 252, part 1, p 1-23.

GISCHLER, E., 2006, Sedimentation on Rasdhoo and Ari atolls, Maldives, Indian Ocean: Facies, v. 52, p. 341-360.

GISCHLER, E., 1994, Sedimentation on three Caribbean atolls: Glovers Reef, Lighthouse Reef and Turneffe Islands, Belize: Facies, v. 31, p. 243-254.

GISCHLER, E., AND LOMANDO, A.J., 2005, Offshore sedimentary facies of a modern carbonate ramp, Kuwait, northwestern Arabian-Persian Gulf: Facies, v. 50, p. 443-462.

GISCHLER, E., DIETRICH, S., HARRIS, D., WEBSTER, J.M., AND GINSBURG, R.N., 2013, A comparative study of modern carbonate mud in reefs and carbonate platforms: Sedimentary Geology, v. 292, p. 36–55.

GRIMALT, J.O., YRUELA, I., SAIZ-JIMENEZ, C., TOJA, J., DELEEUW, J.W., AND ALBAIGES, J., 1991, Sedimentary lipid biogeochemistry of an hypereutrophic alkaline lagoon: Geochimica et Cosmochimica Acta, v. 55, p. 2555-2577.

HALLOCK P., AND GLENN, E.C. (1986) Larger foraminifera: A tool for paleoenvironmental analysis of Cenozoic carbonate depositional facies. PALAIOS 1:55–64.

HERRERA-SILVEIRA, J. A., MEDINA-GOMEZ, I., ARANDA-CIREROL, N., ZALDIVAR, A., RAMIREZ, J., AND TREJO, J., 2002, Trophic status in coastal waters of the Yucatan Peninsula (SE, Mexico) using water quality indicators, in Breddia, C.A., ed., Coastal Environments: WIT Press, p. 351-359.

JAHNERT, R., DE PAULA, O., COLLINS, L., STROBACH, E., PEVZNER, R., 2012, Evolution of a coquina barrier in Shark Bay, Australia by GPR imaging: Architecture of a Holocene reservoir analog: Sedimentary Geology, v. 281, p. 50-74.

JAMES, N.P., 1997, The cool-water carbonate depositional realm, in James, N.P., and Clarke, J.A.D., eds., Cool-water Carbonates: SEPM Special Publication, v. 56, p. 1-20.

KERANS, C., AND FITCHEN, W.M., 1995, Sequence hierarchy and facies architecture of a carbonate ramp system: San Andres Formation of Algerita Escarpment and Western Guadalupe Mountains, West Texas and New Mexico: The University of Texas at Austin, Bureau of Economic Geology Report of Investigations No. 235, 86 p.

KERANS, C., AND LOUCKS, R. G., 2002. Stratigraphic setting and controls on occurrence of high-energy carbonate beach deposits: Lower Cretaceous of the Gulf of Mexico: GCAGS Transactions, v. 52, p. 517-526.

KILLOPS, S.D., AND KILLOPS, V. J., (Eds.) 2005, Introduction to Organic Geochemistry: Blackwell Publishing, Massachusetts, p. 166-245.

LEES, A., 1975 Possible influence of salinity and temperature on modern shelf carbonate sedimentation: Marine Geology, v. 19, p. 159-198.

LITTLER, M. M., LITTLER, D. S., LAPOINTE, B. E., 1988, A comparison of nutrient- and light-limited photosynthesis in psammophytic versus epilithic forms of Halimeda (Caulerpales, Halimedaceae) from the Bahamas: Coral Reefs, v. 6, p. 219-225.

LOGAN, B.W., 1969, Carbonate Sediments and Reefs, Yucatan Shelf, Mexico: American Association of Petroleum Geologists Memoir 11, p. 355.

MACINTYRE, I. G. AND ARONSON, R. B., 2006, Lithified and unlithified Mg-calcite precipitates in tropical reef environments: Journal of Sedimentary Research, v. 76, p. 81–90.

MARSHALL, J. F. AND DAVIES, P. J., *Halimeda* bioherms of the northern Great Barrier Reef: Coral Reefs, v. 76, p. 81–90.

MATTHEWS, R. K., 1966, Genesis of recent lime mud in southern British Honduras: Journal of Sedimentary Petrology, v. 6, p. 139-148.

MERINO, M., 1997, Upwelling on the Yucatan Shelf: Hydrographic evidence: Journal of Marine Systems v. 13, p. 101–121.

MILLIMAN, J.D., FREILE, D., STEINE, R.P., AND WILBER, R.J., 1993, Great Bahama Bank muds: Mostly inorganically precipitated, mostly exported: Journal of Sedimentary Petrology, v. 63, p. 589-595.

MUTTI, M., AND HALLOCK, P., 2003, Carbonate systems along nutrient and temperature gradients: some sedimentological and geochemical constraints: International Journal of Earth Sciences, v. 92, p. 465-475.

O'CONNELL, L., AND JAMES, N.P., 2015, Composition and Genesis of Temperate, Shallow-Marine Carbonate Muds: Spencer Gulf, South Australia: Journal of Sedimentary Research, v. 85, p. 1275-1291.

PARRISH, J.T., ZIEGLER, A.M., AND HUMPHREVILLE, R.E., 1983, Paleozoic paleo-geography and upwelling, in Thiede, J., and Suess, E., eds., Coastal Upwelling: Its Sediment Record, v. B: New York, Plenum Press, p. 553-578.

PURDY, E.G., 1963, Recent calcium carbonate facies of the Great Bahama Bank. 2. Sedimentary facies: Journal of Geology, v. 71, p. 472-497.

PURDY, E.G., AND GISCHLER, E., 2003, The Belize margin revisited: 1. Holocene marine facies.- International Journal of Earth Sciences, v. 92: p. 532-551.

PURSER, B.H., (Ed.) 1973, The Persian Gulf: Holocene Carbonate Sedimentation and Diagenesis in a Shallow Epicontinental Sea: Springer-Verlag, Berlin, p. 471.

RANKEY, E.C., 2014, Contrasts between wave- and tide-dominated oolitic systems: Holocene of Crooked-Acklins Platform, southern Bahamas: Facies, 60, 405-428.

RANKEY, E.C., AND REEDER, S.L., 2010, Controls on platform-scale patterns of surface sediments, shallow Holocene platforms, Bahamas: Sedimentology, v. 57, p. 1545-1565.

RANKEY, E.C., REEDER, S.L., GARZA-PEREZ, J.R., 2011, Controls on links between geomorphical and surface sedimentological variability: Aitutaki and Maupiti atolls, South Pacific Ocean: Journal of Sedimentary Research, v. 81, p. 885-900.

REEDER, S.L., AND RANKEY, E.C., 2008, Relations between sediments and tidal flows in ooid shoals, Bahamas: Journal of Sedimentary Research, v. 78, p. 175-186.

REIJMER, J.J.G., SWART, P.K., BAUCH, T. OTTO, R., REUNING, L., ROTH, S., AND ZECHEL, S., 2009, A re-evaluation of facies on Great Bahama Bank I: New facies maps of western Great Bahama Bank: *in* Perspectives in Carbonate Geology: A Tribute to the Career of Robert Nathan Ginsburg, Swart, P.K., Eberli, G.P., McKenzie, J.A., eds., IAS Special Publication 41. Blackwell, Oxford, p. 29-46.

RUIZ-RENTERIA F., 1979, Upwelling north of the Yucatan Peninsula: MSc. Thesis. Texas A&M University. p. 86.

RUPPEL, S.C., AND WARD, B.W., 2013, Outcrop-based characterization of the Leonardian carbonate platform in west Texas: Implications for sequence-stratigraphic styles in the Lower Permian: AAPG Bulletin, v. 97, p. 223-250.

SCHLAGER, W., 2003, Benthic carbonate factories of the Phanerozoic: International Journal of Earth Sciences, v. 92, p. 445-464.

TUDHOPE, A.W., SCOFFIN, T.P., STODDART, D.R., AND WOODROFFE, C.D.. 1985, Sediments of Suwarrow Atoll: Proceedings of the 5th International Coral Reef Symposium, v. 6, p. 611–616.

WATNEY, W. L., GUY, W. J., AND BYRNES, A. P., 2001, Characterization of the Mississippian chat in south-central Kansas: AAPG Bulletin, v. 85, p. 85–113.

WESTPHAL, H, HALFAR, J., AND FREIWALD, A., 2010, Heterozoan carbonates in subtropical and tropical settings in the present and past: International Journal of Earth Sciences, v. 99, p. S153-S169.

Figures

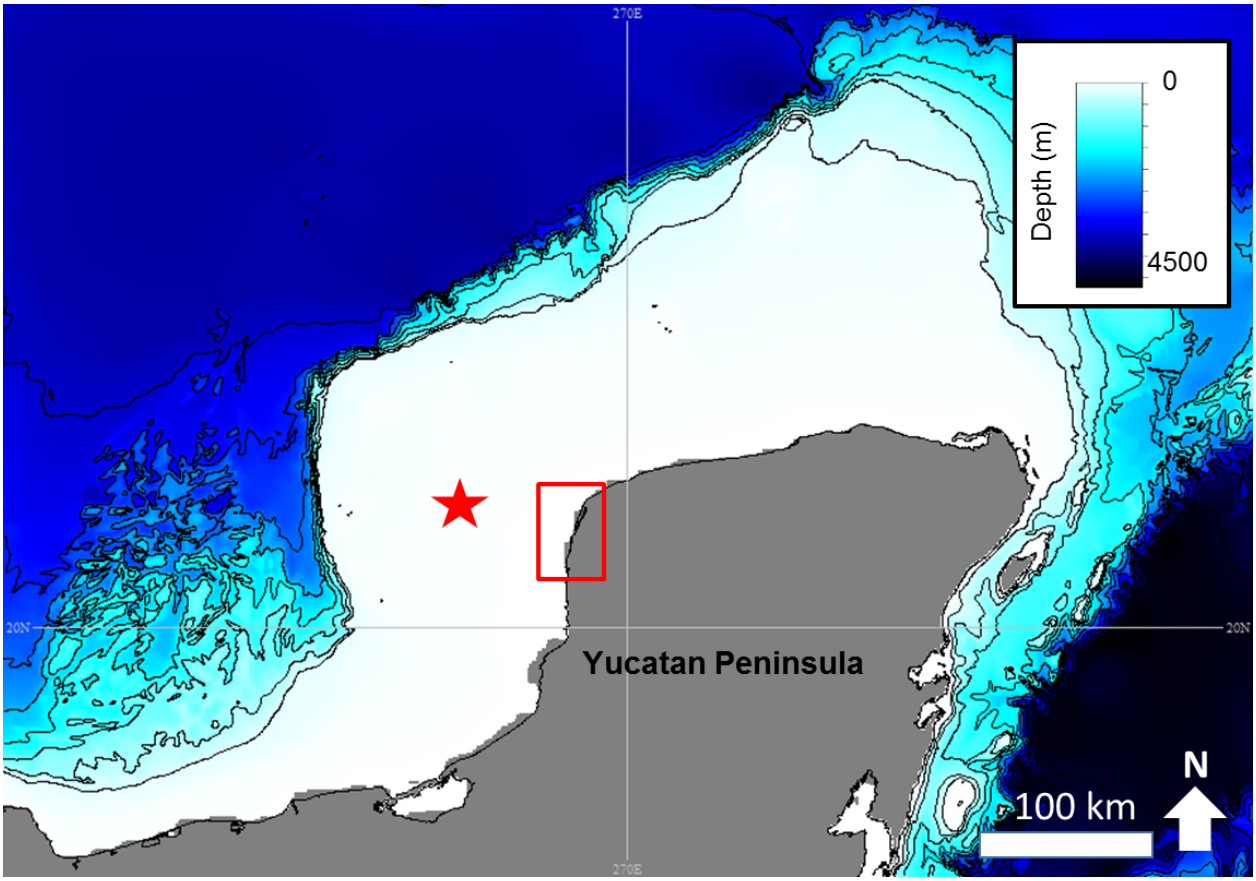

Fig. 1. Map of the Yucatan ramp, also known as Campeche Bank, extending roughly 150-350 km basinward into the Gulf of Mexico (GOM) from the Yucatan Peninsula (land, shown in grey). Study area indicated by red rectangle and red star shows location of wave data (Figure 3).

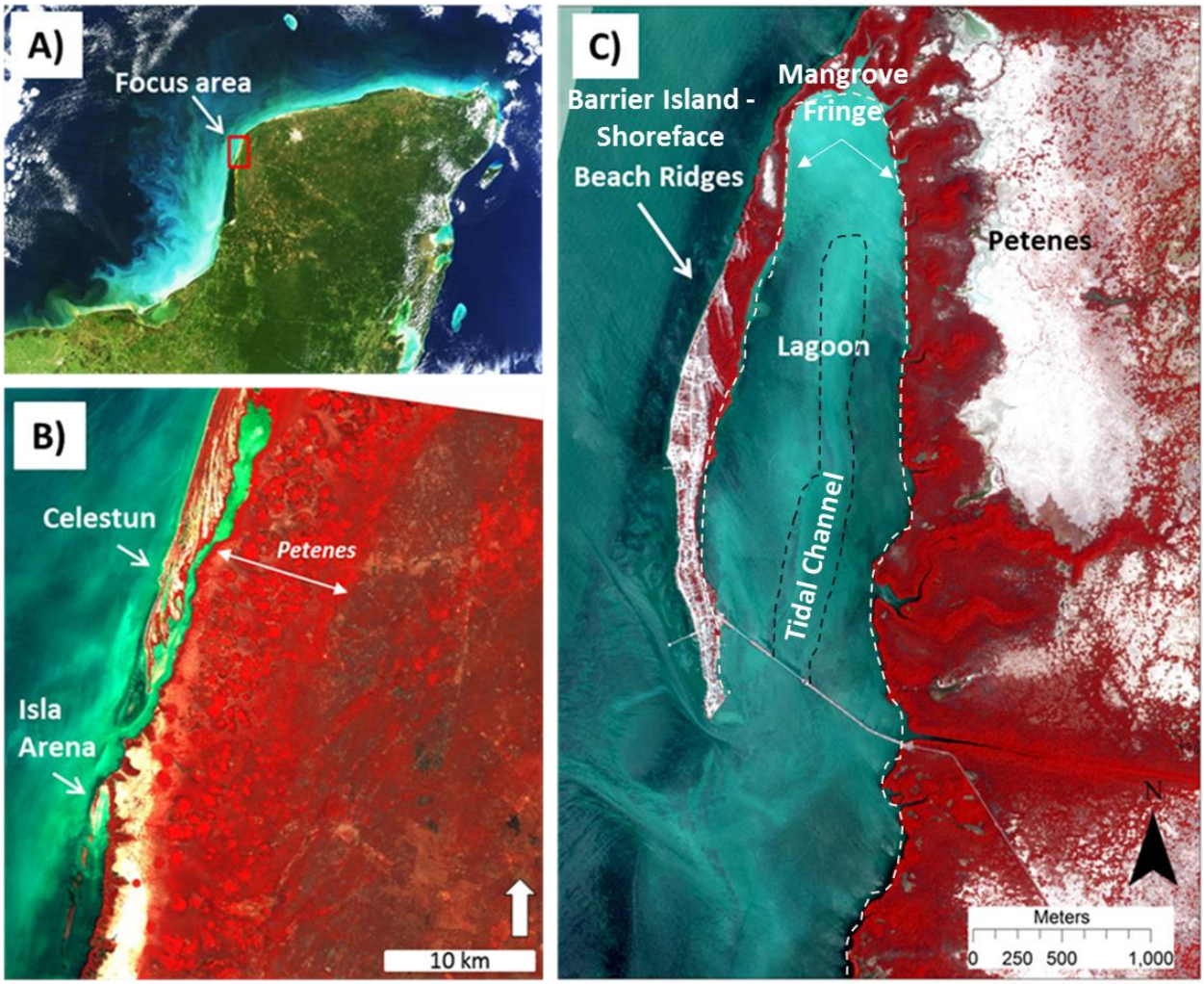

Fig. 2. Remote sensing images of the northwestern Yucatan peninsula. A) Location of study area on the Yucatan Peninsula. Note the turbid offshore water. B) Study areas on the western peninsular flank. Note that Isla Arena (to the south) includes comparable, but smaller-scale, beach ridges than those north, near Celestun (to the north). C) Focus area near Isla Arena showing the shoreface-barrier island made up of beach ridges, the lagoon, a N-S trending tidal channel located in the middle of the lagoon, mangrove fringe, and freshwater marsh, the "Petenes."

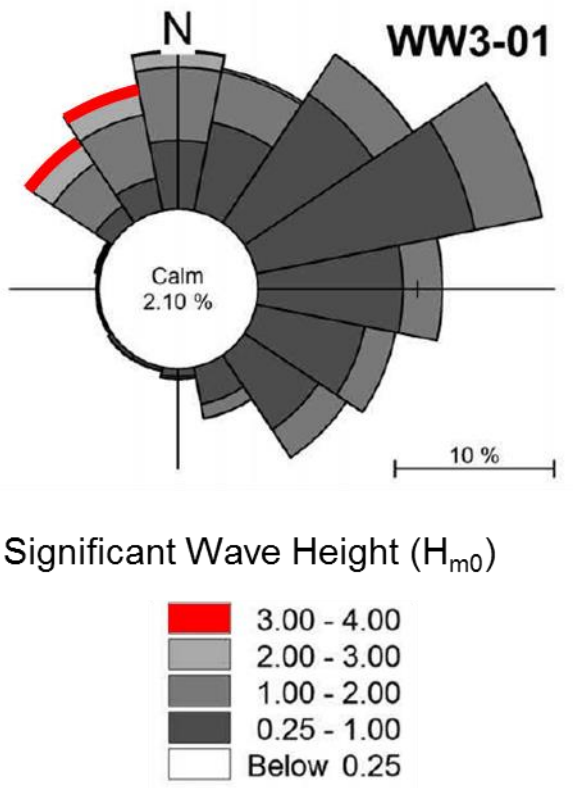

Fig. 3. Wave rose diagram showing significant wave heights, the frequency with which they occur, and the direction from which they originate. Note that the most frequent waves are from the NE. In contrast, the largest waves (3-4 m, highlighted with red color) are from the NW. These waves, associated with the passage of fronts ("Nortes"), occur mainly in the winter months, rather than occurring throughout the year. Location from which data are collected is indicated by red star in Figure 1. Modified from Appendini et al., 2012.

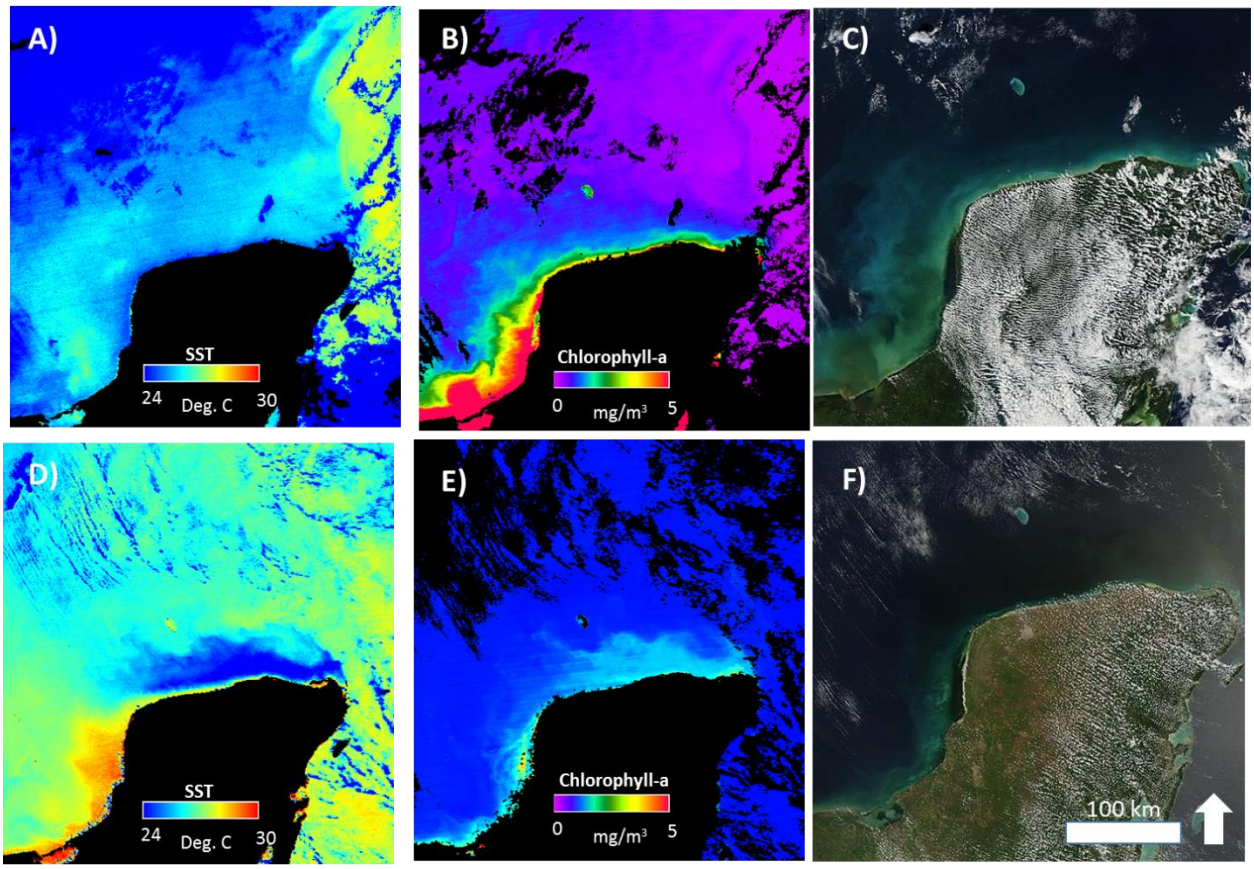

Fig. 4. Paired sea surface temperature (SST), chlorophyll-a levels (Chl-a), and turbidity illustrating variability off the coast of the Yucatan Peninsula. A-C) Representative winter conditions, January 5, 2014, A) SST showing waters 24-26°C along the Yucatan coast. B) Chl-a levels indicating elevated nutrients along the western Yucatan coast. C) Visible image emphasizing high turbidity along the north and western Yucatan coast, caused by plankton blooms. D-F) Illustrative spring-summer conditions, May 17, 2015. D) SST illustrating cooler (upwelled) waters (≤24°C) off the northern Yucatan coast. E) Chl-a levels along the coast; nutrient levels are elevated (up to 2 mg/m^3), but lower than in the winter (Part B). F) Turbidity along the coast of the Yucatan; tubidity is less during the spring than in the winter.

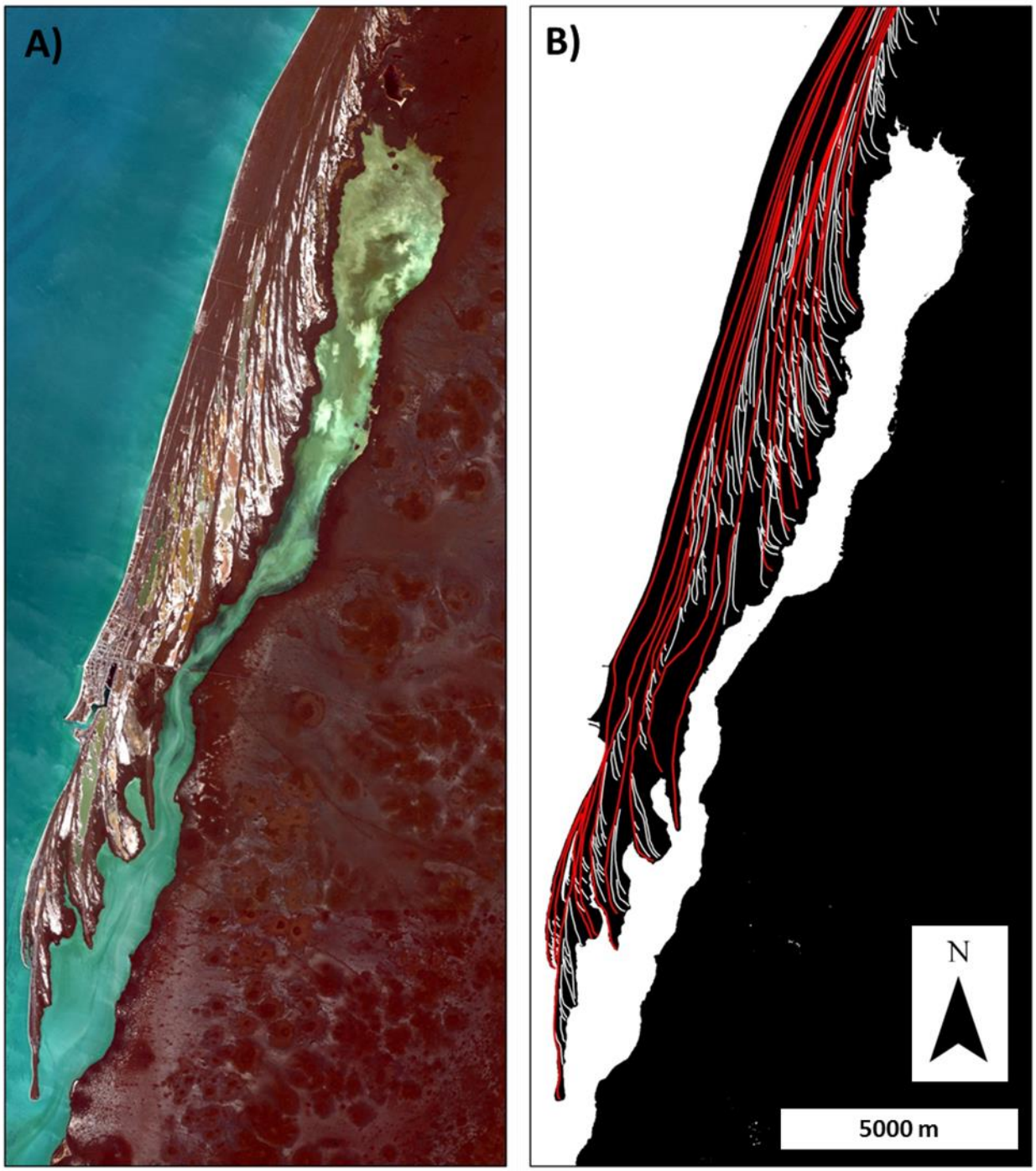

Fig. 5. Paired satellite image and interpretative diagram of beach-ridge barrier island complex near Celestun. A) Uninterpreted remote sensing image. Note that the complex is ~30 km long, up to 3 km wide, and is made up of well-developed southward diverging planform beach ridges. The beach ridge complex protects a low-energy lagoon in its lee. B) Interpretive image, with barrier island beach ridges outlined to show depositional trends and geometries. The largest, first-order beach ridges (recognized by merging of smaller sets) are outlined in red; Shorter second-order spits (which merge into the first-order beach ridges), outlined in white. See text for discussion.

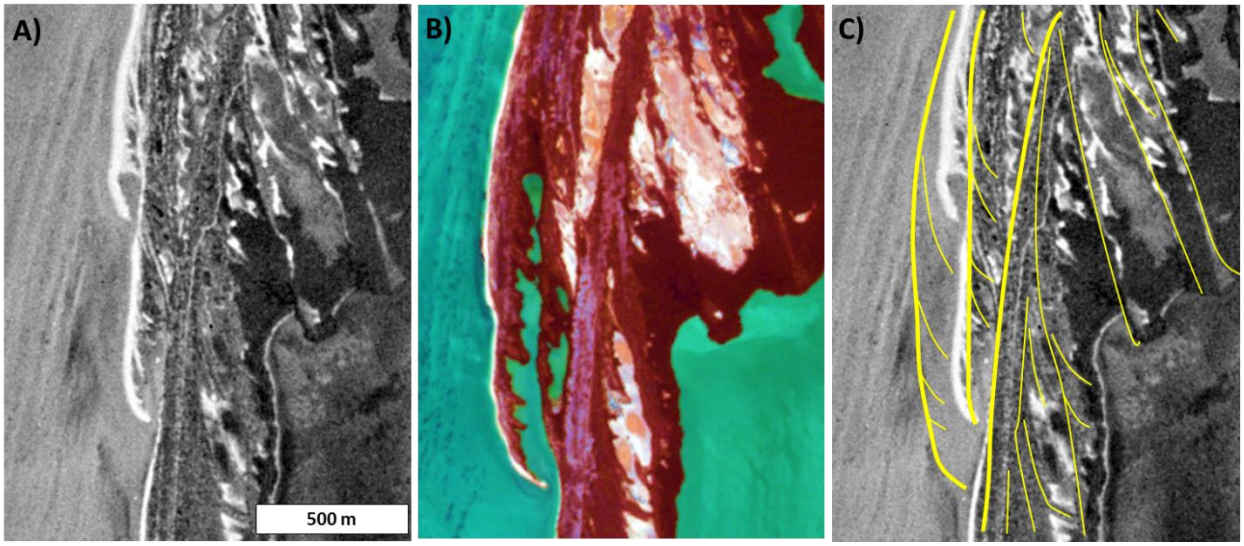

Fig. 6. Temporal evolution of the barrier island system just south of the town of Celestun, 1978-2011. A) 1978 aerial photo of the barrier island coastline and beach ridges. B) 2011 image of the barrier island coastline and beach ridges near Celestun. C) The 1978 image with the 2011 extent of the beach ridges indicated by yellow lines. Comparison reveals southward (alongshore) progradation of a beach ridge up to 1 km in 33 years (an average of 30 m/yr), resulting in a net shoreline progradation (offshore) of up to 200 m.

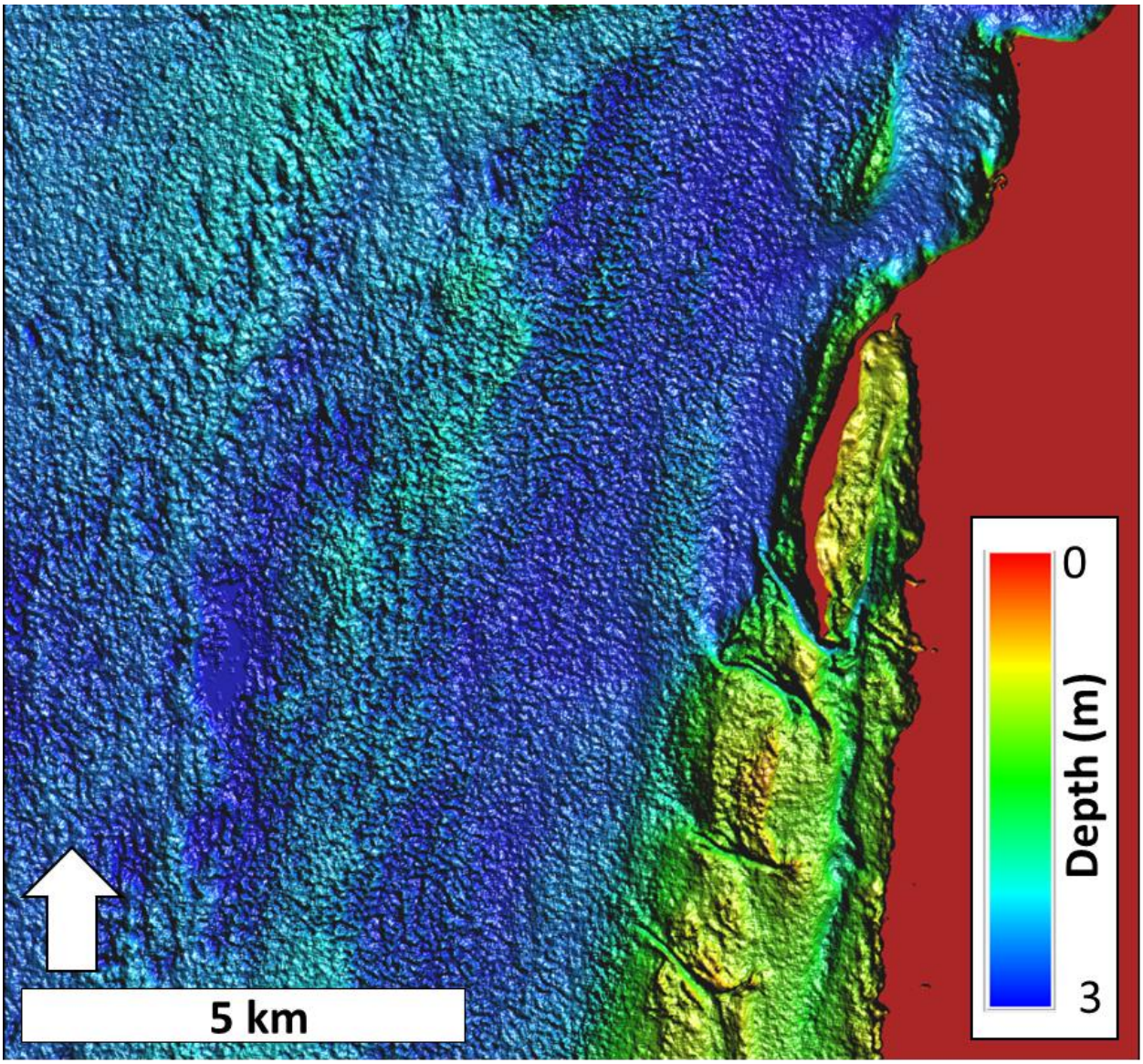

Fig. 7. Satellite-predicted bathymetry of the study area at Isla Arena. The supratidal to terrestrial barrier island-foreshore and Petenes systems are shown in red. The intertidal to shallow subtidal lagoon has a fairly consistent depth trend – shallower near the mangrove fringe and up-dip (N) within the lagoon, and deeper towards the center (e.g., N-S trending tidal channel) and to the south, towards the open ocean. Water depths within the lagoon are less than 2 m. Grainy bathymetric highs continue southwest of the barrier island with cross-cutting channels. Water depths increase subtly westward (up to 3 m, 8 km offshore), but not simply or linearly. In these subtidal offshore areas, sea grass beds and *Halimeda* meadows are associated with local subtle highs (<1 m relief). (Map generated by Rodrigo Garza-Perez).

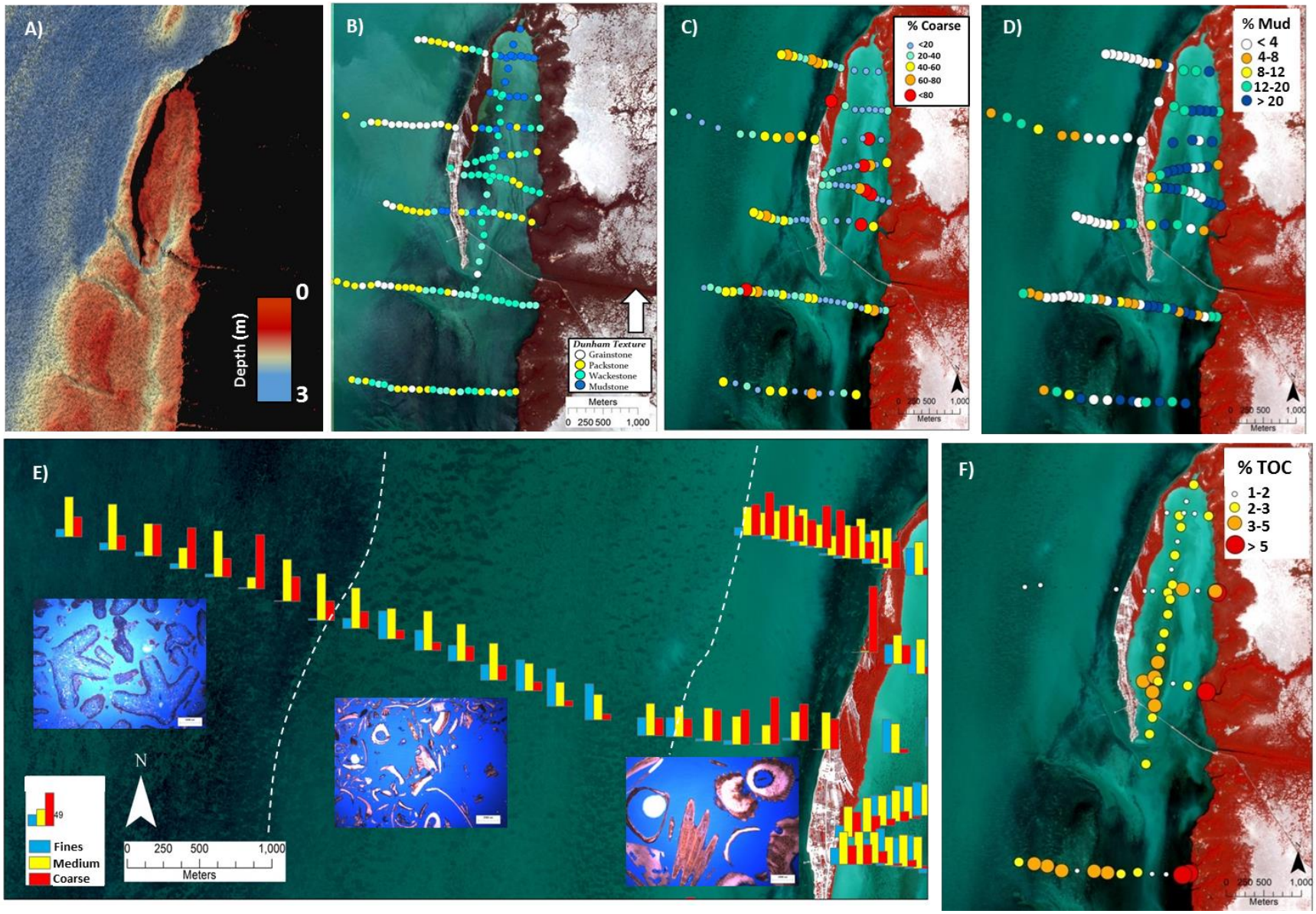
A)
Depth (m)
0
3
B)
Dunham Texture
Grainstone
Packstone
Wackestone
Mudstone
Meters
0 250 500 1,000
C)
% Coarse
<20
20-40
40-60
60-80
<80
D)
% Mud
< 4
4-8
8-12
12-20
> 20
E)
N
Fines
Medium
Coarse
0 250 500 1,000
Meters
F)
% TOC
1-2
2-3
3-5
> 5

Fig. 8. (previous page) Sedimentologic and geomorphologic trends. A) Bathymetry. B) Dunham texture of surficial sediment. C) Percent coarse fraction; note coarse-grained sediment of N-S trending tidal channel in center of lagoon. D) Percent mud fraction; note mud-dominated lagoon, with exception of tidal channel. E) Representative foreshore-offshore transect showing the distribution of coarse, medium, and fine sediment, and representative thin sections. Transect extends ~7 km offshore. Note the general shore-parallel trends of molluscan-rich medium-coarse sediment nearshore, a central more mud-rich zone, and an outer zone with abundant *Halimeda*. F) Percent total organic carbon (TOC). Note that organic carbon is most abundant in the lagoon, and least abundant offshore.

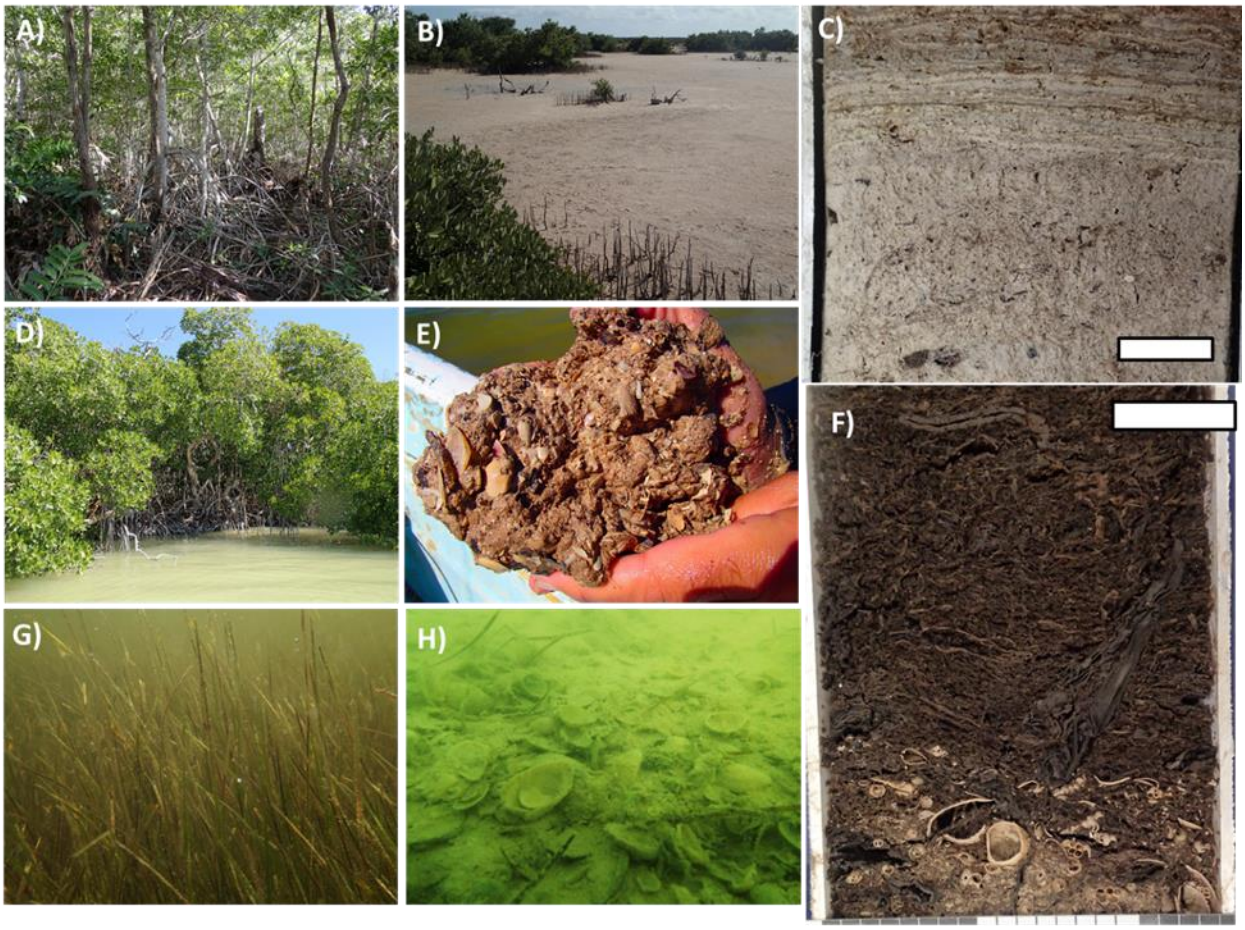

Fig. 9. Field photographs and facies photos illustrating geomorphic and sedimentologic variability of the "Petenes" and lagoon. A) White mangrove-dominated zone of the "Petenes." This zone extends between 4-10 km inland (eastward) from the coastline in the Isla Arena area. B) Black mangrove-dominated supratidal "Petenes" marsh zone. C) Core from the marsh zone (cf. Figure 9B) showing the microbial laminations, organic matter, and scattered gastropod shell fragments (Scale = 2 cm). D) Mangrove-dominated flank of the lagoon. E) Representative sediment along the mangrove fringe, consisting of very poorly sorted muddy to fine sand and gravel. Dominant sediment particles are bivalves and gastropods, with common barnacles. F) Core taken from the mangrove fringe showing a gastropod fragments overlain by a dark, spongy, peat layer (Scale = 2 cm). The mangrove fringe is the most organic matter -rich geomorphic element in the study area (TOC = ~15%). G) Seagrass-covered bottom of the lagoon. H) Underwater photo of whole and fragmented bivalve shells that make up most of the sediment in the N-S trending tidal channel.

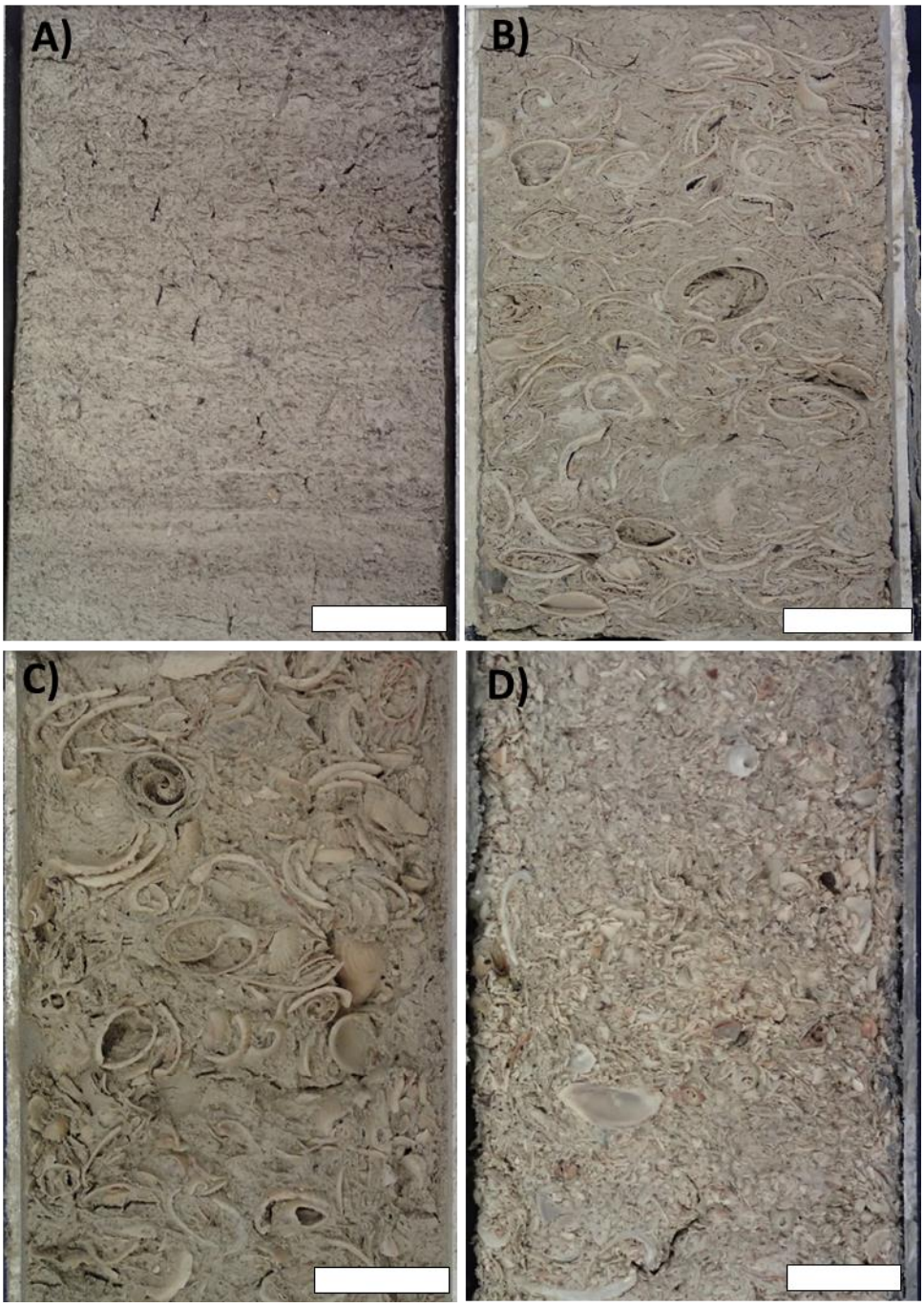

Fig. 10. Representative core photos from different geomorphic elements. A) Representative core from the lagoon showing vaguely laminated wackestone and seagrass roots. B) Molluscan packstone, representative of the sediment from the flank of the coarse tidal channel in the center of the lagoon. Sediment in the tidal channel consists mostly of whole and partly fragmented mollusc fragments. C) Molluscan mud-lean packstone from ~50 m outboard of the barrier island foreshore. Note the large, mostly unbroken molluscs. D) Fine packstone from the grainy bathymetric high south of the island. Grains are more fragmented and abraided than grains in the foreshore core (part C) and near the tidal channel within the lagoon (part B).

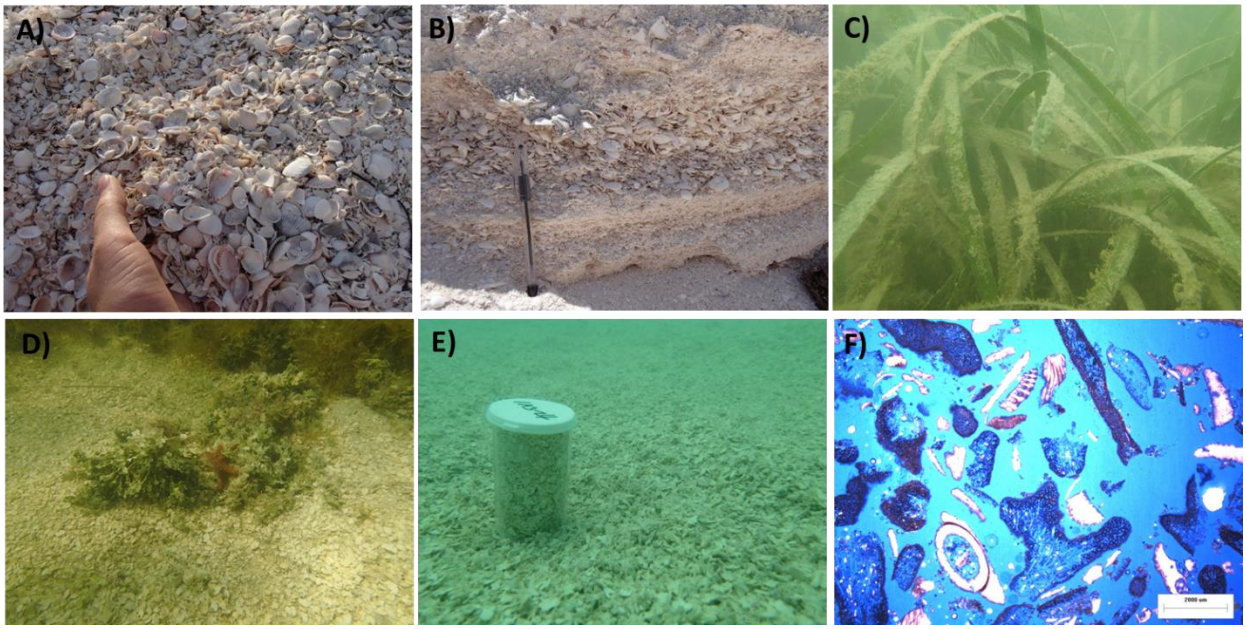

Fig. 11. Field photos and bottom types showing sedimentologic variability among the beach ridge, shoreface, and offshore. A) Beach ridge ridge sediment, composed of gravel to coarse sand with no mud. B) The wall of a trench showing coarse - fine layering with whole and fragmented bivalves. C) Thalassia-covered subtidal bottom. D) Live *Halimeda* and *Halimeda* gravel. E) Close-up view of bare *Halimeda* bottom. *Halimeda* gravel makes up most of the sediment >3 km offshore in the study area. F) A representative thin section from the offshore area, showing a mix of fragmented bivalves and *Halimeda* fragments. Scale is 2 mm.

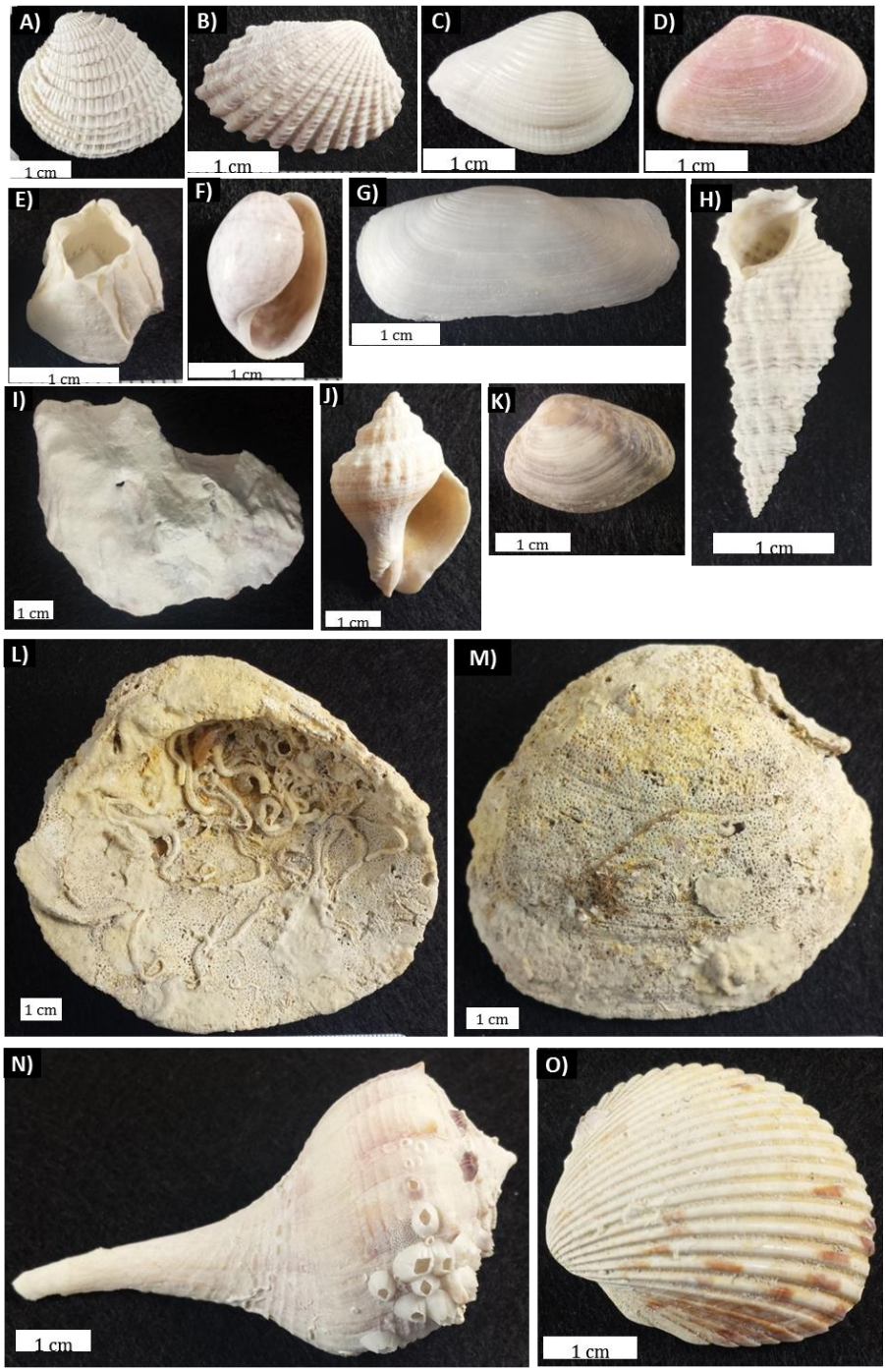

Fig. 12. Molluscan Assemblages A) Chione cancellata. B) Cardita floridana. C) Anomalocardia auberiana. D) Tellina alternata. E) Amphibalanus improvisus. F) Bulla occidentalis. G) Tagelus plebeius. H) Cerithium. I) Crassostrea Rhizophorae. J) Melongena bispinosa abundant near mangrove fringe. K) Unidentified lagoonal bivalve abundant near mangrove fringe. L) Underside of Mercenaria mercenaria showing encrusted serpulid worm tubes. M) Top of Mercenaria mercenaria showing borings made by Clionidae, a red, boring sponge. N) Busycon coarctatum with encrusted barnacles, Amphibalanus improvisus. O) Dinocardium Robustum

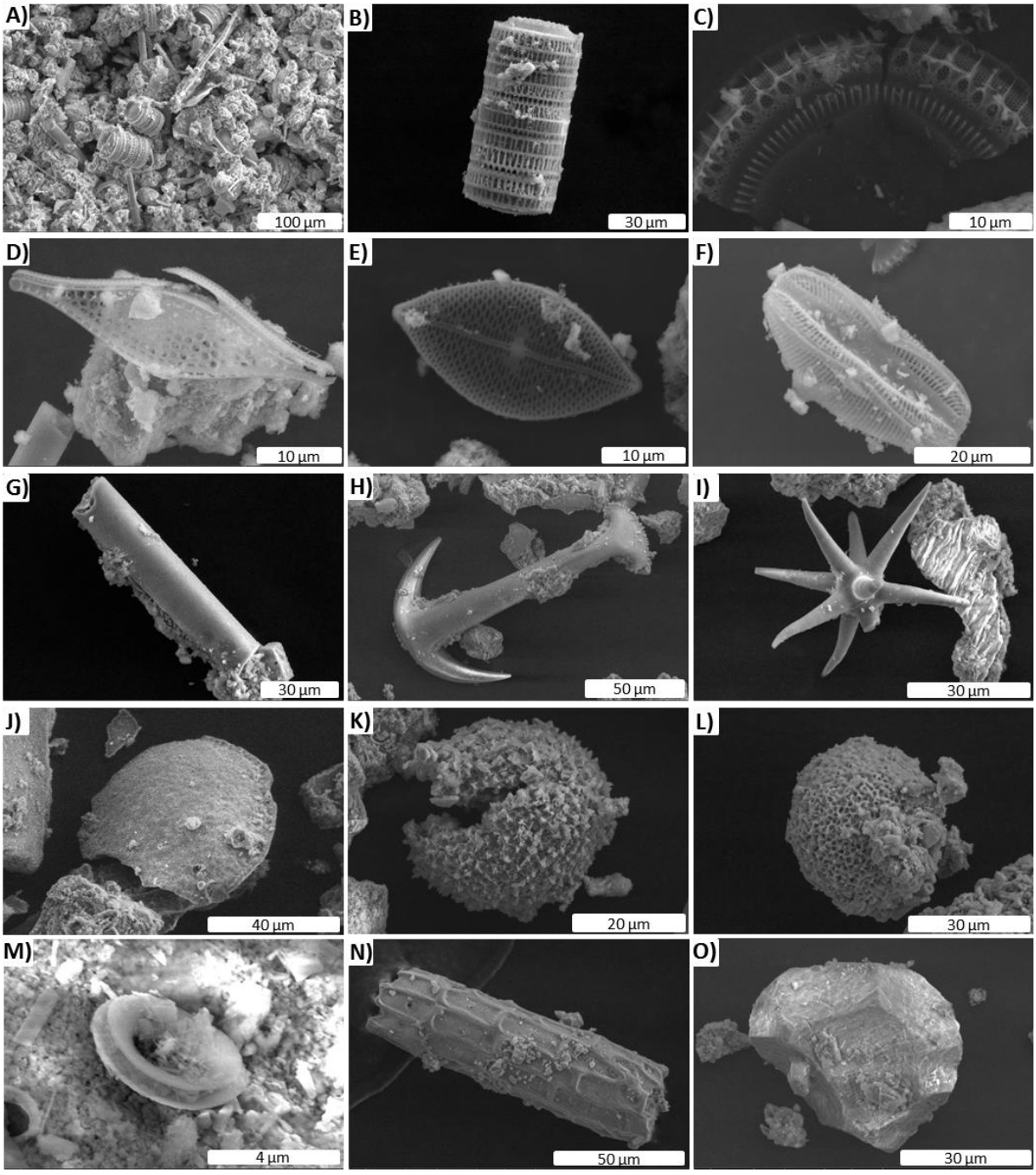

Fig. 13. Biosiliceous particles found in the mud-sized (< 63µm) portion of the sediment. A) Representative SEM snapshot of the mud-sized sediment constituents. Note abundance of diatoms, sponge spicules, and non-descript particles. B-F) Diatoms E) Delphineis minutissim (maybe??). G-I) Sponge sicules. J-L) Dinoflagellate cysts. M) Coccolithophore plate. N) Echinoid fragment. O) Clionid sponge boring.

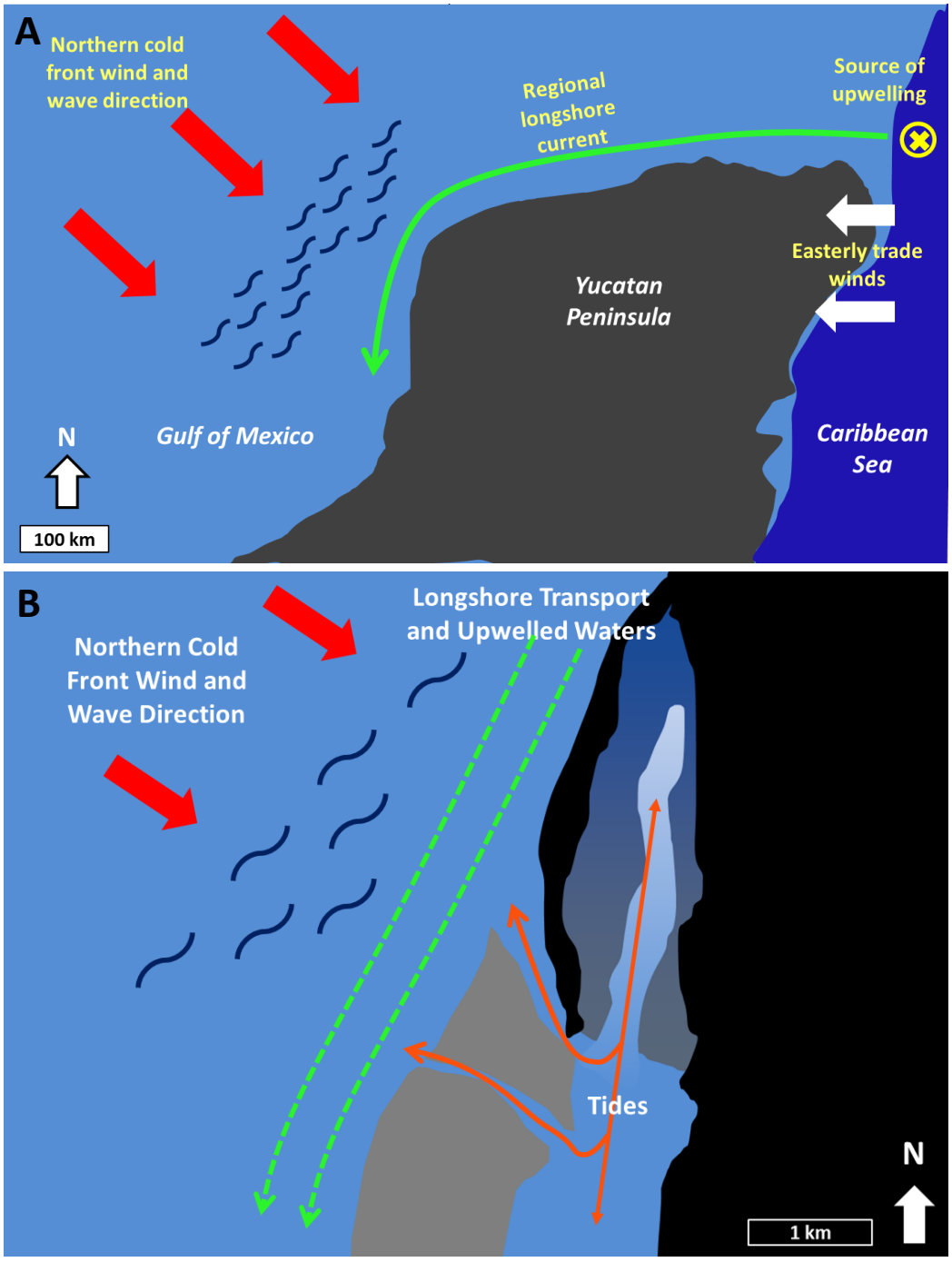

Fig. 14. Conceptual model illustrating the physical and chemical oceanographic processes influencing the northwestern Yucatan shelf. A) Regional setting. With respect to the easterly trade winds, the northwestern Yucatan is on the leeward side of the peninsula. Upwelling originates off the northeastern Yucatan coast and upwelled water is carried westward along the northern coast, and southward along the western coast. The northern cold front winds generate large waves (H_s >2.5 m) from November to March. B) Local setting, Isla Arena study area. Longshore currents driven by the regional current and northern cold fronts carry cooler waters

and nutrients southward along the western coast. The deposition and accumulation of sediment results in the southward progradation of the barrier island spit, which in turn contributes to the formation of a lower energy, semi-restricted, mud-dominated lagoon on the leeward flank of the barrier island. The tides of this micro-tidal system carry open-marine water and offshore sediment into the lagoon, where finer-grained sediment from offshore settles out in the quieter setting. In the most restricted part of the lagoon, at the northern end, sediment texture transitions to more dominantly mudstone to wackestone.

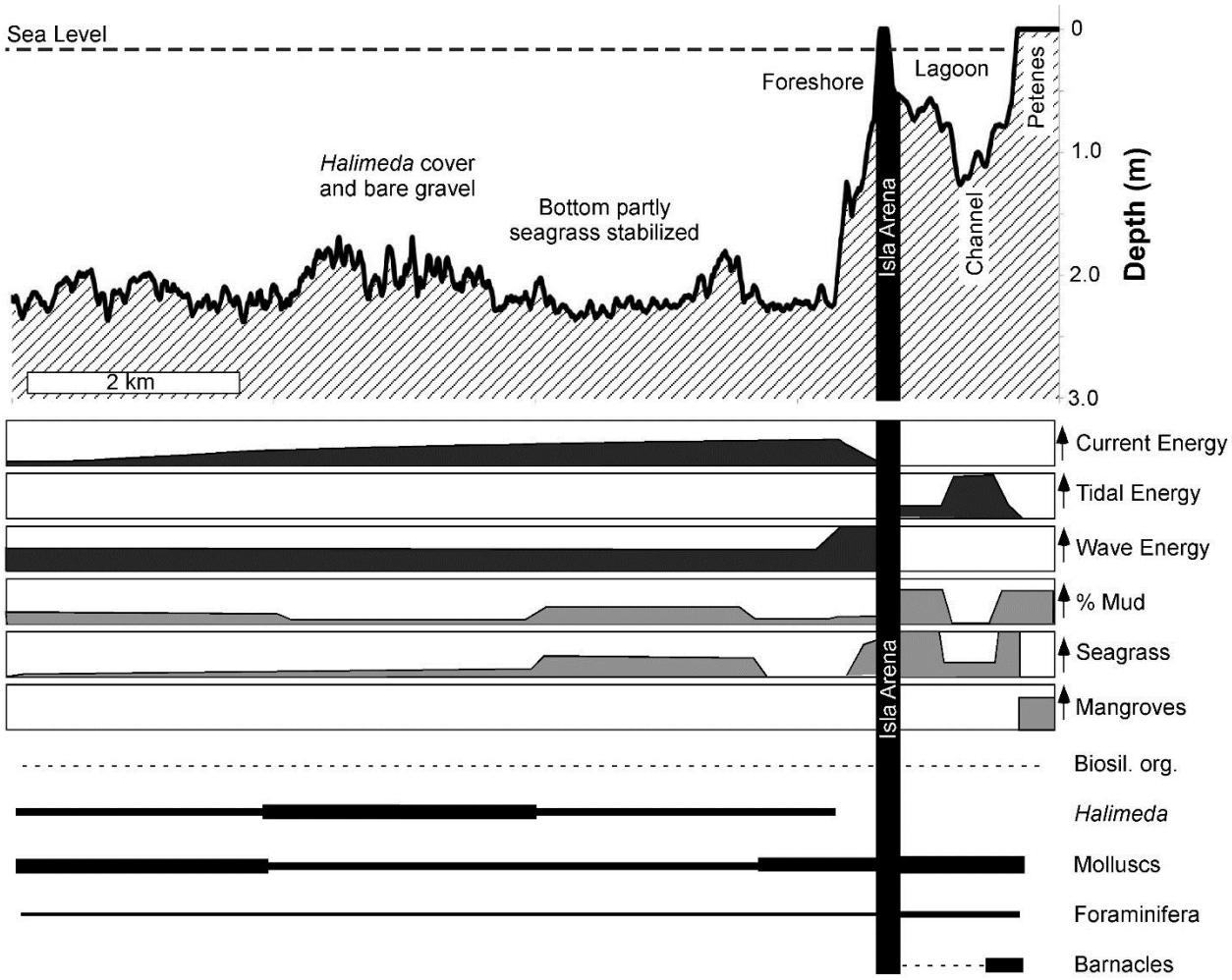

Fig. 15. Schematic diagram illustrating relative impacts of processes, mud content, selected vegetation, the relative abundance of some dominant or important macrofauna. The offshore regions are characterized by zones with 1) live *Halimeda* cover and *Halimeda* gravel with little to no mud; 2) a higher proportion of mud and fines stabilized by luxuriant seagrass cover; and 3) whole and fragmented molluscan sand to gravel. The upper shoreface is the area of highest wave energy and longshore sediment transport facilitates the formation and southward progradation of molluscan coquina beach ridges. Leeward of the barrier island is a shallow subtidal to intertidal, mud-rich (>20%) lagoon with exception of a bivalve- and gastropod- gravel-rich tidal channel that runs down the axis of the lagoon. Macrofauna in the lagoon consists of bivalves, gastropods, foraminifera, and barnacles.

Appendix 1 – Organic Matter Characterization

This study attempted to understand the variability in distribution of organic matter type throughout the lagoon, beach ridges, and offshore by collecting samples and performing Gas chromatography and mass spectrometry (GCMS) to identify and characterize sources of organic matter. Broad generalizations were made from the data; however, although understanding the subtle changes of the sources of organic matter would be interesting and useful, identifying specific sources of organic matter was outside the scope of the project.

Methods

Samples were initially prepared and extracted using the Bligh-Dyer method. Approximately five grams of the sample was placed in a VOA vial with 12 mL of 1:2 dichloromethane:methanol (v:v) and vortexed. Three mL of dichloromethane and 3 mL of deionized (DI) water were added to the mixture and mixed gently. To further aid and continue the separation process, 1 mL of dichoromethane and DI water were alternately added. A pipet was used to remove the extract and reacted with activate copper to remove elemental sulfur present in the extract. The extract was then evaporated to dryness. One mL of dichloromethane was added to the vial containing the extract, in addition to 5-10 mL of methanol containing 5% hydrochloric acid. The sample was left overnight in a sand bath at 70˚C. Afterwards, 10 mL of hexane was added to the vial, the top layer was extracted into another VOA vial using a pipet and evaporated almost to dryness (~1 mL). The extract was moved into a GC vial and was splitlessly injected into the gas chromatograph through an inlet port heated to 150˚C. The gas chromatograph was heated from 40˚C to 130˚C at a rate of 20˚C per minute, and then ramped at 5˚C per minute to 350˚C, where it was held for 3 min. Analytes were then analyzed on a

ThermoFinnigan Trace GC-DSQ in full-scan mode positive ion mode. Compounds were identified by using their relative retention times and mass spectral data.

The Bligh-Dyer Extraction method did not extract enough organic material and detection using GCMS was minimal and identification was not possible as the peaks in the mass spectral data were too small to separate signal from noise. Microwave extraction as a second method was used as a second attempt to characterize the organic matter. Approximately 5 g of sample were 5 g of sample was measured into a Teflon vessel, and 24 mL of 1:1 dichloromethane:methanol (v:v) was added to each vessel. These vessels were then extracted in the 800 W microwave accelerated reaction system (MARS Xpress); the temperature was ramped to 100˚C for 5 min, where it was held for 30 min, and then cooled back to room temperature for 15 min. The solvent-extracted organic material was then vacuum filtered to remove the sediment from the sample, and reacted with activate copper to remove elemental sulfur present in the extracts. Sulfur content was high enough in the sample that it was often necessary to repeat this clean-up step. The extract was then injected into the gas chromatograph using the same method and parameters as described in the previous paragraph. Compounds were identified by using their relative retention times and mass spectral data.

Results

To identify the type, source and distribution of organic matter, samples representative of the variability across the Isla Arena area were analyzed by gas chromatography/mass spectroscopy (GC/MS). The analysis, as seen in the total ion current (TIC) traces, reveal a variety of organic compounds. For purposes of this study, the most important type of compound is *n*-alkanes, whose distribution can be a general indicator of source input. For example, low-

molecular-weight compounds < C_{15} are generally interpreted to indicate a bacterial source, middle-range compounds between approximately C_{19} and C_{25} suggest algal inputs, and high-molecular-weight compounds > C_{25} are considered to represent terrestrial plant input (Brocks and Summons, 2003; Peters et al., 2005).

The TIC chromatograms suggest similarities among most samples, and some differences. For example, the m/z 85 trace from ~1.5 km offshore (west) of Isla Arena (IA3-O13) reveal *n*-alkanes characteristic of modern algae and bacterial biomarkers. This offshore sample contained no aged organic material. Similarly, the m/z 85 trace for a sample from south of the Isla Arena, ~2 km offshore from the mainland (IA7-22), includes a broadly comparable mix of fresh algal and bacterial biomarkers, but no aged material. Unlike sample IA3-O13, however, the m/z 191 indicates the presence of plant triterpenes which reflects the traces of terrestrial plants. In sharp contrast to these samples from offshore, a sample from an organic rich (TOC = 7.39) portion of a core from the supratidal mangrove marsh zone suggests the presence of fatty acids, indicating fresh organic matter that has not had sufficient time to break down. Likewise, the sample includes plant triterpenes, representative of terrestrial organic matter. Fossil plant biomarkers are also found in addition to the modern plant biomarkers showing that organic matter is being preserved in the older, buried portions of sediment.

The results of these analyses illustrate that, for the most part, most samples from across the area have the same general TIC patterns and organic matter biomarkers with one marked exception – samples taken in or near the mangrove fringe have TICs that display a wider array of preserved organic material, both terrestrial and marine sourced, than the rest of the samples from the lagoon and the offshore areas, which is consistent with the findings that the samples from the mangrove fringe have the highest TOC values (~15%).

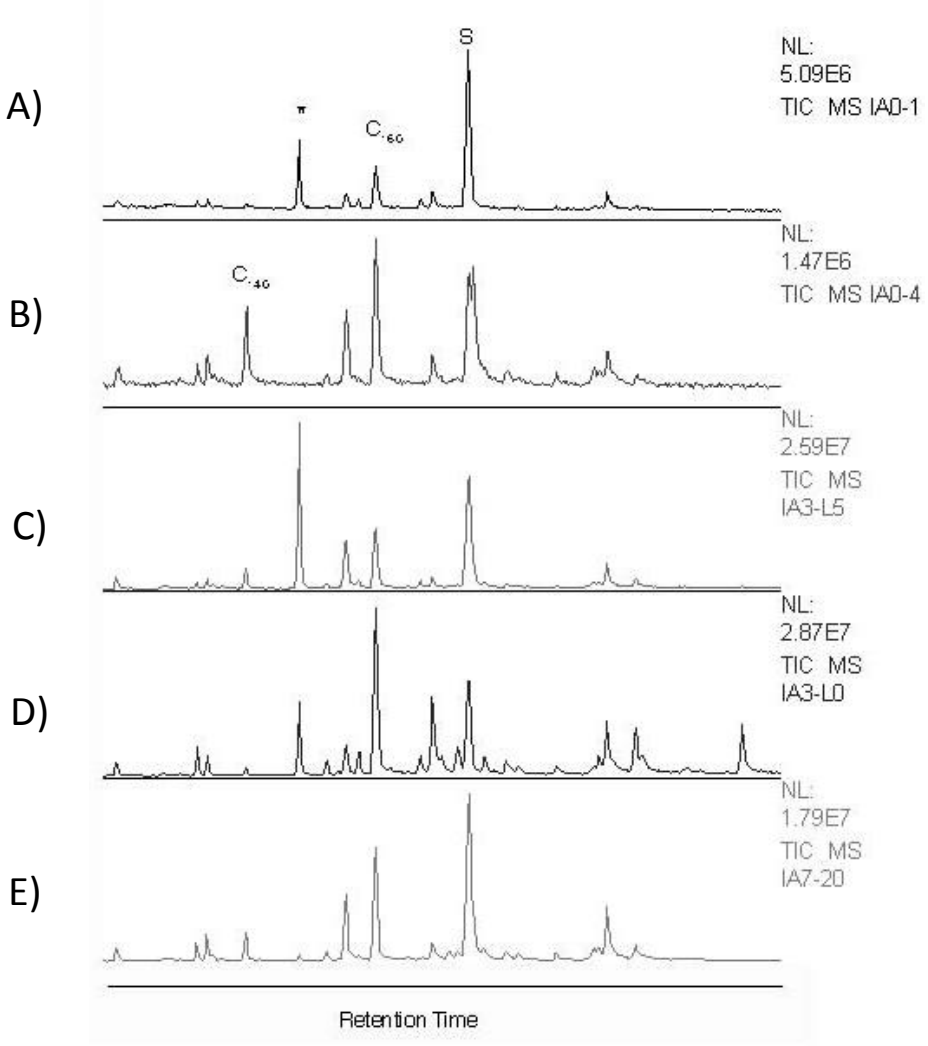

Total Ion Chromatrogams for representative samples throughout the study area. A) IA0-1 from the northernmost, most restricted part of the lagoon. B) IA0-4 from the center of the lagoon. C) IA3-L5 also from approximately from the center of the lagoon but further south than IA0-4 and nearer to the gravelly tidal channel within the lagoon. D) IA3-LO sample taken from the eastern mangrove fringe; note more peaks representing a wider variety of organic matter sources. E) IA7-20 representative of the offshore.